

Effects of boundary conditions on magnetization switching in kinetic Ising models of nanoscale ferromagnets

Howard L. Richards*

Department of Physics,

University of Tokyo, Hongo, Bunkyo-ku, Tokyo 113, Japan

and Department of Solid State Physics,

Risø National Laboratory, DK-4000 Roskilde, Denmark

and Center for Materials Research and Technology, Department of Physics,

and Supercomputer Computations Research Institute,

Florida State University, Tallahassee, Florida 32306-3016

M. Kolesik†

Supercomputer Computations Research Institute, Florida State University, Tallahassee, Florida

32306-4052

Per-Anker Lindgård&

Department of Solid State Physics,

Risø National Laboratory, DK-4000 Roskilde, Denmark

Per Arne Rikvold‡

Department of Fundamental Sciences, Faculty of Integrated Human Studies

Kyoto University, Kyoto 606-01, Japan

and Center for Materials Research and Technology, Department of Physics,

and Supercomputer Computations Research Institute,

Florida State University, Tallahassee, Florida 32306-3016

M. A. Novotny§

Supercomputer Computations Research Institute,

Florida State University, Tallahassee, Florida 32306-4052

and Department of Electrical Engineering,

2525 Pottsdamer Street, Florida A&M University–Florida State University,

Tallahassee, Florida 32310-6046

(May 2, 2019)

Abstract

Magnetization switching in highly anisotropic single-domain ferromagnets has been previously shown to be qualitatively described by the droplet theory of metastable decay and simulations of two-dimensional kinetic Ising systems with *periodic* boundary conditions. In this article we consider the effects of boundary conditions on the switching phenomena. A rich range of behaviors is predicted by droplet theory: the specific mechanism by which switching occurs depends on the structure of the boundary, the particle size, the temperature, and the strength of the applied field. The theory predicts the existence of a peak in the switching field as a function of system size in both systems with periodic boundary conditions and in systems with boundaries. The size of the peak is strongly dependent on the boundary effects. It is generally reduced by open boundary conditions, and in some cases it disappears if the boundaries are too favorable towards nucleation. However, we also demonstrate conditions under which the peak remains discernible. This peak arises as a purely dynamic effect and is not related to the possible existence of multiple domains. We illustrate the predictions of droplet theory by Monte Carlo simulations of two-dimensional Ising systems with various system shapes and boundary conditions.

PACS Number(s): 75.50.Tt, 75.40.Mg, 64.60.Qb, 05.50.+q.

I. INTRODUCTION

The next generation of high-density magnetic recording media should have much higher storage densities without sacrificing large coercivity. The experimentally observed non-monotonic dependence of the coercivity on particle diameter (see, e.g., Ref. 1) implies that the optimum size of ferromagnetic grains for use in recording media is small enough to be single-domain but large enough to be nonsuperparamagnetic.^{2,3} The purpose of this paper is to extend earlier studies⁴⁻⁸ which used Ising systems to model the nonequilibrium statistical mechanics of magnetization reversal. Specifically, we investigate the dependence of the switching field, which is usually measured in static or slowly increasing fields, on the boundary conditions. We show that the boundary conditions strongly influence switching phenomena for weak applied fields and small systems, and that this influence is observable in the switching field. Some preliminary results of the present study have been published in Ref. 9.

A. Micromagnetic theories of magnetization reversal

The simplest theory of magnetization reversal in single-domain ferromagnets is due to Néel¹⁰ and Brown.¹¹ In order to avoid an energy barrier due to exchange interactions between atomic moments with unlike orientations, Néel-Brown theory assumes uniform rotation of all the atomic moments in the system. The remaining barrier is caused by magnetic anisotropy,² which may have contributions from both the local crystalline environment and from the macroscopic shape of the particle. Anisotropy makes it energetically favorable for each atomic moment to be aligned along one or more “easy” axes. Because the magnetization of the entire system rotates uniformly, the free-energy barrier ΔF separating the metastable (magnetization antiparallel to the applied field) phase from the stable (magnetization parallel to the applied field) phase is proportional to the volume of the particle. The lifetime τ of the metastable phase is related to ΔF by the Van’t Hoff-Arrhenius¹² equation

$$\tau \propto \exp(\beta\Delta F), \quad (1)$$

where $\beta^{-1} \equiv k_B T$ is the temperature in units of energy. In what follows, we use units in which $k_B = 1$. Another specific prediction³ from the uniform rotation model is that the switching field increases with system size as

$$H_{\text{sw}} = \begin{cases} \approx 0 & \text{for } N \leq N_P \\ H_0 \left(1 - \sqrt{\frac{N_P}{N}} \right) & \text{for } N_P \leq N \leq N_{\text{MD}} \end{cases} \quad (2)$$

for a three-dimensional particle. Here H_0 is the asymptotic value of the switching field; N is the particle volume; N_P is a volume depending on the anisotropy, the waiting time τ , the saturation magnetic moment of the particle, and the temperature; and N_{MD} is the volume above which the equilibrium magnetic structure of the particle consists of two or more domains. For $N > N_{\text{MD}}$, the switching field decreases, since magnetic reversal can take place by means of domain-wall motion.

Detailed descriptions of both the static and dynamic properties of fine ferromagnetic grains have typically been formulated from micromagnetic models,¹³ of which Néel-Brown theory is a particularly simple case. This method involves coarse-graining the physical lattice onto a computational lattice and then solving the partial differential equations for the evolution of the coarse-grained magnetic structures. Although micromagnetics provides a good treatment for the anisotropy and demagnetizing fields,¹⁴ it treats thermal effects rather crudely, usually just by making the domain-wall energy temperature-dependent. A somewhat better approximation for thermal fluctuations within the underlying differential equations is to include a Langevin noise term.¹⁵ Yet another possibility is a mean-field type approach to switching behavior.¹⁶ A better treatment for thermal and time-dependent effects is Monte Carlo simulations (see, e.g., Refs. 4–8, 17–22). Even when the physical phenomena can be accurately simulated, however, it will be difficult to understand the results without an adequate theoretical basis. It is the purpose of this paper to extend that theoretical basis and support it with Monte Carlo simulations for the Ising model with a variety of boundary conditions.

B. Droplet Theory of Magnetization Reversal

For highly anisotropic systems, magnetization reversal occurs not by means of uniform rotation, but by the nucleation and growth of *nonequilibrium droplets* of the stable magnetic phase.²³ The coupling between the magnetic field and the magnetization within a droplet favors growth of the droplet, but the interface tension of the droplet favors shrinkage. A droplet for which these two forces are balanced is termed a critical droplet.

Kinetic nearest-neighbor Ising models form a class of highly anisotropic model systems that have become popular subjects for Monte Carlo simulations of metastable decay (see Ref. 24 and references cited therein). The reasons for this are easy to understand. A great variety of exact results have been obtained for the equilibrium two-dimensional Ising model in zero field.^{25–29} As a nontrivial model for which a number of exact results are known, it has become a favorite of researchers in statistical mechanics, and it has been a standard in investigations of universality,³⁰ finite-size scaling,³¹ and various approximation schemes, such as series expansions.³² *Kinetic* Ising models with a variety of stochastic spin-flip dynamics have proven useful as simple but nontrivial models for the study and testing of ideas in nonequilibrium statistical mechanics, such as dynamic universality and critical exponents,^{33,34} and metastability.³⁵

For these reasons, kinetic nearest-neighbor Ising models have been extensively studied as prototypes for switching dynamics in highly anisotropic systems. Square- and cubic-lattice Ising systems with periodic boundary conditions have been used to study grain-size effects in ferroelectric switching.^{36,37} Magnetization reversal in elongated ferromagnetic particles has been studied with a one-dimensional model,³⁸ and a triangular-lattice Ising model with mean-field magnetostatic interactions has been shown to reproduce well the switching dynamics in Dy/Fe ultrathin films.¹⁷ Square-lattice kinetic Ising models with free boundaries were simulated by Mélin,¹⁸ and Serena and García^{19,20} performed Monte Carlo simulations on square-lattice Ising systems with free circular boundaries. In earlier work^{4,6–8} we have considered kinetic Ising models with periodic boundary conditions as models for magnetization switching in single-domain ferromagnetic nanoparticles. In the present paper

we extend our analytical and numerical study to the effects of nucleation at the particle boundary.

C. Phenomena Affecting Magnetism at Boundaries

It is well known that the physics of surfaces is far more complicated than one might expect based on simple cross-sections of bulk material.³⁹ For instance, atoms near the system boundary may move from their bulk-crystalline positions in order to lower the free energy, a process known as reconstruction. Also, the chemical environment of the system boundary may be very different from the bulk, since the boundary provides sites for possible chemisorption. Furthermore, the reduction in symmetry often changes the magnetic anisotropy at the boundary. This is clearly seen in some thin films which become perpendicularly magnetized if their thickness is less than some critical value.⁴⁰

The various boundary effects can influence each other.⁴¹ For instance, the ferromagnetic metal nickel undergoes reconstruction when oxygen,^{42,43} nitrogen,^{44,45} carbon,^{43,46,47} sulfur,^{43,48} or alkali metals⁴⁹ chemisorb on its surface. It has been observed both experimentally^{50,51} and computationally⁵² that clean nickel undergoes a surface structural phase transition at the Curie temperature of bulk nickel. Likewise, the electronic changes which cause bonding in chemisorption can lead to changes in magnetic properties.⁴¹ For example, an oxygen atom adsorbing on Ni(100) reduces the local magnetic moments on the nickel atoms in its vicinity.⁵³

The breaking of translational symmetry by surfaces can also affect magnetic properties at surfaces directly, as it disrupts the spin-wave spectrum and other long-ranged excitations.³⁹ This effect can be particularly pronounced in nanoscale particles, since the ratio of “boundary” atoms to “bulk” atoms can be significant.⁵⁴

As a result of the wide variety of physical phenomena which can affect magnetism at the surfaces of single-domain grains, it is clear that an adequate understanding of magnetization switching in real ferromagnetic grains requires an understanding of the effects of fairly general boundary conditions. In this study we therefore consider in detail the effects of several specific modifications to the system boundary.

D. Experimental Observations of Nanoscale Magnets

Fine ferromagnetic grains have been studied for many years. For instance, in Ref. 1 Kneller and Luborsky measured the coercivity and remanence of iron and iron-cobalt particles. They found that the coercivity measurements agreed well with Eq. (2) for particles sufficiently small to be single-domain, and that the coercivity rapidly drops to the small bulk value for multi-domain particles. Until recently, however, such particles could be studied experimentally only in powders, which made it difficult to differentiate the statistical properties of single-grain switching from effects resulting from distributions in particle sizes, compositions, and local environments, or from interactions between grains.

Recently a variety of techniques have become available which permit one to resolve the magnetic properties of isolated, well-characterized, single-domain ferromagnets.⁵⁵ One such technique is magnetic force microscopy (MFM).⁵⁶ Several experiments were important for

inspiring our interest in a possible connection between magnetization switching in single-domain magnetic grains and metastability in kinetic Ising models.

In Ref. 57, Chang et al. used MFM to study the switching field of isolated barium ferrite fine particles. The shapes of the particles (determined by atomic force microscopy) were used to determine the demagnetizing field for each particle, which was subtracted from the observed switching field. The resulting effective field has a peak with respect to the particle diameter somewhat similar in appearance to that which was reported in Ref. 1, although in this case it is believed that the grains remain single-domain, since the peak occurs at a grain diameter of about 55 nm. Thus it is difficult to explain the peak in switching field reported in Ref. 57 in terms of Néel-Brown theory. In Refs. 4 and 6 we showed that a purely dynamic crossover in the switching mechanism can cause such a peak in systems with periodic boundary conditions. A central aim of the present study is to understand how more realistic boundary conditions affect this peak.

MFM measurements on individual iron particles⁵⁸ showed that as the particle diameters increase from 20 nm to 70 nm, the switching fields decrease. The angular dependence of the switching field indicates that the magnetization reversal is not coherent at small field angles.

Size effects somewhat similar to those in barium ferrite particles have also been observed in nanoscale single-domain Ni bars.⁵⁹ The switching field of an isolated bar initially increases with increasing bar width (the length of bars used in the experiment was fixed), then reaches a maximum at a width of 55 nm, and decreases with further bar-width increase. As the authors of that study note, the decrease for wide bars probably occurs because the bars change from single-domain to multidomain with increasing width, since only bars of width less than 150 nm are single-domain. However, one may speculate that the switching-field peak and the decrease in the 50 — 100 nm range could originate from dynamic effects such as those found in computer simulations of Ising-like systems.^{4,6}

The magnetization reversal mode in long Ni columns was studied in Ref. 60. A weak dependence of the switching field on the radius of the column was found, which is not consistent with the curling mode. Nucleation at the particle ends was suggested to be responsible for this behavior. Measurements of switching fields and their histograms for similar Ni wires with smaller diameters (< 100 nm) give evidence that the magnetization reversal in narrow wires results from a nucleation and growth processes.⁶¹

Peaks in the switching field with respect to the particle diameter have typically been attributed to a crossover to a multidomain initial condition. However, if a field significantly stronger than the demagnetizing field is initially applied parallel to the particle magnetization, the probability of even a very small domain existing as an initial condition when the field is reversed can be made quite small, even for particles that are multidomain in equilibrium at zero field. It is possible that these conditions were achieved in a recent experiment by Yang et al.,⁶² in which they applied a 2T initializing field to nanocrystalline powders of the ferrimagnet LiFe_5O_8 . Particularly intriguing is the fact that the ratio between the peak value of H_{sw} and the value for the largest particle size they report (860 nm) is approximately 1.7. By comparing the dependence of the lifetime on the exponential part of the nucleation rate, it can be shown that for a three-dimensional periodic system that ratio should be 2, at least in the limit of long waiting times.⁸ It is worth pointing out that surface effects are a major concern of Ref. 62, so it may be that surface nucleation is sufficiently discouraged to

cause the particles to be similar to periodic systems. Unfortunately, the large polydispersity in their powder samples makes detailed interpretation difficult. Microscopic measurements of isolated, well-characterized particles under similar conditions would therefore be highly desirable.

Another set of experiments involved the measurement of the probability P that the magnetization in $\gamma\text{-Fe}_2\text{O}_3$ ^{63–65} single-domain particles is switched by an opposing field. The probability P was measured as a function of applied field for a constant waiting time, and as a function of time for a constant applied field. The experiments show that the mean switching time (or lifetime) τ depends strongly on the strength of the applied field H , which indicates that droplet nucleation is occurring — if switching were taking place by domain wall motion, τ would depend on H much more weakly.

Magnetization switching in nanoscale particles is often driven by a desire to investigate macroscopic quantum tunneling. In a series of papers,^{66–69} Wernsdorfer and co-authors studied the dynamics of magnetization reversal at very low temperatures, which perhaps span the temperature regimes of macroscopic quantum tunneling and thermal activation. They measured switching fields and their probability distributions, as well as the probability for switching at constant applied magnetic field in cobalt nanoparticles.⁶⁸ They suggested that the magnetization switching is triggered by a nucleation process and that the reversal mechanism in one small particle is more complex than the model of uniform rotation. They also observed that the topological fluctuations of the magnetization state, due to sample imperfections, affect the switching properties at low temperatures.^{67,69}

For some materials, such as thin films of Fe on a sapphire substrate, patterned single-crystal islands can be made small enough that they will be single domain, and interactions with the substrate can yield a single easy axis. In fact, these islands remain single domain over a wide range of sizes and shapes, and their easy axes lie in the same directions independently of the island shape.⁷⁰ Consequently, the Ising model is a reasonable first description of such materials.

The experimental evidence discussed above indicates both that nucleation is an important aspect of magnetization switching in nanoscale ferromagnets, and that heterogeneous nucleation at boundaries and defects plays at least as important a role as homogeneous nucleation in the particle bulk. It provides the motivation for the extension of our previous work on bulk nucleation to consider nucleation at the particle boundaries, which we present in this paper.

E. Organization of the Article

The organization of the rest of this paper is as follows. In Sec. II we describe the boundary conditions and dynamics used. In Sec. III we briefly review droplet theory for systems with periodic boundary conditions. These ideas, with some extensions, are necessary for a proper understanding of droplet theory in systems with restricted geometry. In Sec. IV we apply the concepts of droplet theory to systems with external boundaries. We particularly concentrate on the dependence of the switching field on the particle size and boundary conditions. In Sec. V we present our Monte Carlo results and compare them with our theoretical predictions. Finally, in Sec. VI we summarize our results.

II. DESCRIPTION OF THE MODEL SYSTEMS

A. Boundary Conditions

In order to facilitate study of boundary effects such as those mentioned in Subsec. IC, as well as the effects of a simply truncated lattice, we have modified the square-lattice Ising Hamiltonian (see Subsec. IIB below) by allowing the exchange interaction and the applied field to be modified at the boundary. This type of modification has yielded a variety of both numerical results⁷¹ and exact results⁷² for the Ising model in equilibrium — particularly for the boundary magnetization and the boundary free energy in the absence of a magnetic field applied to the bulk.^{25,28} We introduce three types of systems.

- i) Square systems of side L with periodic boundary conditions in only the crystal axis \hat{y} direction are referred to as *semiperiodic systems*; such systems have the topology of a cylinder. Quantities related specifically to these system are denoted by the superscript \square in order to distinguish them from their counterparts for other types of systems.
- ii) Systems consisting of all sites lying within a circle of diameter L centered midway between sites [i.e., at $(\frac{1}{2}, \frac{1}{2})$ if there is a site at both $(0,0)$ and $(1,1)$ on a square lattice] and with open boundary conditions are referred to as *circular systems*. We use the superscript \odot to denote quantities specific to the circular lattices.
- iii) Systems consisting of all sites lying within an octagon of width L , centered midway between sites and with periodic boundary conditions in no direction are referred to as *octagonal systems*. In an attempt to make the boundary more uniform, half the nearest-neighbor bonds on the edges of the system parallel to the \hat{x} - and \hat{y} axes are omitted. See Fig. 1.

B. The Hamiltonian

The Ising model is defined by the Hamiltonian

$$\mathcal{H}_0 = -J \sum_{\langle i,j \rangle} s_i s_j - H \sum_i s_i , \quad (3)$$

where $s_i = \pm 1$ is the z component of the dimensionless magnetization of the atom (spin) at site i , $J > 0$ is the ferromagnetic exchange interaction, and H is the applied magnetic field times the single-spin magnetic moment. The sums $\sum_{\langle i,j \rangle}$ and \sum_i run over all nearest-neighbor pairs and all sites on a lattice, respectively. The dimensionless system magnetization is given by

$$m = N^{-1} \sum_i s_i , \quad (4)$$

where N is the total number of sites in the system. The lattice constant is set to unity. In this article we consider different shapes and boundary conditions for the *system*, but the underlying lattice is always taken to be square. For the reader's convenience, we note that the critical temperature of the two-dimensional Ising model is $2J / \log(1 + \sqrt{2}) = 2.26919J$.²⁵

The selection of the Ising model is equivalent to requiring a very large (infinite, in fact) anisotropy constant. Although magnetic materials used in magnetic recording media require comparatively large anisotropy constants,⁷³ the microscopic anisotropy tends to be much smaller than the exchange energy. However, in some applications, such as many thin films, it is convenient to use Ising spins to represent individual grains that are superferromagnetically coupled to make up the system (see, e.g., Refs. 17, 74, 75). If these coupled grains reverse their magnetization through uniform rotation, as in Néel-Brown theory,^{10,11} the anisotropy barrier for a *grain* is the product of the anisotropy barrier for a *single atom* and the grain volume. Thus, although the present work is intended as a step towards a quantitative microscopic theory for nanoscale ferromagnetic particles, it can also be used to describe systems consisting of superferromagnetically coupled grains.

In order to give greater flexibility in dealing with boundaries, we modify the Hamiltonian in Eq. (3) by allowing an additional field H_Σ only at the boundary and an additional coupling J_Σ that connects only nearest-neighbor boundary spins (see Fig. 1). This yields the Hamiltonian

$$\mathcal{H}_\Sigma = \mathcal{H}_0 - J_\Sigma \sum_{\langle i,j \rangle_\Sigma} s_i s_j - H_\Sigma \sum_{i_\Sigma} s_i . \quad (5)$$

The sums $\sum_{\langle i,j \rangle_\Sigma}$ and \sum_{i_Σ} run over all nearest-neighbor pairs of boundary sites and over all boundary sites, respectively.

C. Dynamics and Simulation Methods

The relaxation kinetics are simulated by the single-spin-flip Metropolis dynamic⁷⁶ with updates at randomly chosen sites. The acceptance probability in the Metropolis dynamic for a proposed flip of the spin at site α from s_α to $-s_\alpha$ is defined as

$$W_M(s_\alpha \rightarrow -s_\alpha) = \min[1, \exp(-\beta \Delta E_\alpha)] , \quad (6)$$

where ΔE_α is the energy change due to the flip. A rigorous derivation from microscopic quantum Hamiltonians of the stochastic Glauber dynamic⁷⁷ used in Monte Carlo simulations of Ising models has been established in the thermodynamic limit under certain restrictions.⁷⁸ Both the Glauber and Metropolis algorithms are spatially local dynamics with nonconserved order parameter (the dynamic universality class of Model A in the classification scheme of Hohenberg and Halperin³³) and are therefore expected to differ only in nonuniversal features.

We implement the Metropolis dynamic both by the original, straightforward Metropolis algorithm⁷⁶ and by the “refusal-free” n -fold way algorithm.^{79,80} The n -fold way algorithm is much more efficient than the original Metropolis algorithm at low temperatures, where the latter requires many attempts before a change is made.

The switching process is simulated by starting from an initial state fully magnetized opposite to the applied field, i.e. all spins are in the state $s_i = +1$ and the field $H < 0$. The definition of the lifetime of the metastable state is the mean first-passage time to the cutoff magnetization $m = 0$:

$$\tau = \langle t(m = 0) \rangle . \quad (7)$$

From the lifetimes measured for various strengths of the magnetic field and various system sizes, we numerically determine the switching field, H_{sw} , which is defined as the absolute value of the field required for a system of a given size to exhibit a given lifetime. Thus, the switching field is a function of the temperature, the system size, and of the waiting time. Note that the terms “lifetime” and “waiting time” both stand for the same quantity, τ . We use “lifetime” whenever τ is treated as a dependent variable $\tau(L, H, T)$, and we use “waiting time” when τ is considered an independent variable.

III. DROPLET THEORY FOR HOMOGENEOUS NUCLEATION

In this section we briefly review the droplet theory of nucleation for systems with *periodic* boundary conditions. Most of this material is treated in greater detail in earlier works (see, e.g., Refs. 4, 6–8, 24, 81, 82) but the concepts are needed when we deal with systems with distinct boundaries in the next section, and some of the details we present here have not been published before.

A. General Considerations

The central problem in nucleation theory is to evaluate the free-energy barrier for nucleation of the equilibrium phase, ΔF , which is the free-energy difference between the system containing a single critical fluctuation and the same system in the homogeneous metastable phase. Once this is determined, the dominant field and temperature dependence of the nucleation rate per unit volume is obtained from the Van’t Hoff-Arrhenius relation, Eq. (1). However, in contrast to the mean-field Néel-Brown theory, ΔF is *not* proportional to the system volume.

For the purposes of this paper, it suffices to adopt an approximation in which the system is divided into two distinct regions: a metastable background in which the magnetization approximately equals the zero-field spontaneous magnetization m_{sp} , and a region in which the magnetization is approximately $-m_{\text{sp}}$, parallel to the applied field $H < 0$. This amounts to setting the magnetic susceptibility $\chi=0$ and corresponds to ignoring Gibbs-Thomson type corrections.⁸³ For details on the validity of this approximation for kinetic Ising systems in moderately strong fields, see Refs. 7 and 84.

First we consider the case that the region of stable phase is a single droplet of radius R . For the time being, we do not take into account the fact that the droplet can nucleate anywhere in the system. Such entropy-related contributions to the free energy of a droplet will be included later. The free-energy barrier corresponding to creating a droplet of radius R is then

$$F_{\text{dr}}(R) = \Omega \left[d\sigma R^{d-1} - 2|H|m_{\text{sp}}R^d \right], \quad (8)$$

where σ is the interface tension in a symmetry direction of the lattice and d is the spatial dimension. The quantity Ω is a temperature-dependent factor which gives the volume of a droplet of radius R as ΩR^d ; thus for two-dimensional systems at sufficiently high temperatures that σ is not very anisotropic, $\Omega \approx \pi$. Here and elsewhere in this paper, we set the free energy equal to zero in the uniform *metastable* phase. The maximum of $F_{\text{dr}}(R)$

corresponds to a droplet for which the tendency to grow, due to the coupling of the field and the magnetization, is balanced by the tendency of the droplet to shrink, due to the interface tension. The radius of this critical droplet is

$$R_c = \frac{(d-1)\sigma}{2|H|m_{\text{sp}}} . \quad (9)$$

The free-energy cost of the critical droplet is obtained by using R_c in $F_{\text{dr}}(R)$:

$$\Delta F_{\text{SD}} = \Omega \sigma^d \left(\frac{d-1}{2|H|m_{\text{sp}}} \right)^{d-1} . \quad (10)$$

The subscript SD stands for single-droplet, as will be explained in the next subsection. The free-energy barrier ΔF_{SD} is a function of the temperature T through Ω , σ , and m_{sp} . However, it is *not* dependent on the system size. Later it will become clear that this is an important point.

Inserting ΔF_{SD} into Eq. (1) one gets the dominant contribution to the nucleation rate per unit system volume, $I(T, H)$. A field-theoretical saddle-point calculation gives corrections due to fluctuations about the critical droplet configuration,^{24,85,86} yielding the final result:

$$I(T, H) = B(T)|H|^K \exp \left\{ -\beta \left[\Delta F_{\text{SD}} + O\left(H^{3-d}\right) \right] \right\} , \quad (11)$$

where $B(T)$ is a nonuniversal prefactor. The prefactor exponent K is 3 for the two-dimensional Ising model^{82,85,86} and $-1/3$ for the three-dimensional Ising model,⁸⁶ assuming local diffusional dynamics.

B. Modes of Metastable Decay

Scaling arguments discussed in detail in Refs. 24, 81, and 82 reveal four distinct regions in the space of field and system size, in which the switching proceeds in qualitatively different ways depending on the number of critical droplets which form during the switching process. Below we consider separately the three regimes that are relevant to the range of relatively weak fields studied in the present paper.

The *coexistence* (CE) regime^{81,82} is the part of the L - H plane characterized by systems which are too small to accommodate a critical droplet. Instead, the free-energy barrier separating the stable and metastable phases comes from a “slab” of stable phase,⁸⁷ separated from the metastable background by two interfaces of area L^{d-1} . Since the slab volume can be increased simply by separating these interfaces without increasing the interface area, once such a slab has formed, it almost always continues to grow. The free energy of a “critical” slab is found by equating the interface part of the droplet free energy [the first term in Eq. (8)] with the interfacial free energy of a slab, $2\sigma L^{d-1}$, and inserting the resulting value of R into Eq. (8). The result is:

$$\Delta F_{\text{CE}} = 2 \left[\sigma L^{d-1} - |H|m_{\text{sp}} L^d \left(\frac{2^d}{\Omega d^d} \right)^{\frac{1}{d-1}} \right] . \quad (12)$$

Below we show that the CE regime corresponds to fields weaker than a crossover field proportional to L^{-1} . As a result, ΔF_{CE} depends on L as L^{d-1} . The dominant contribution to the lifetime for slabs is obtained by inserting ΔF_{CE} in Eq. (1). In addition there may be prefactors analogous to those in Eq. (11), but their forms are not known. We therefore obtain the following expression for the lifetime in the CE regime:

$$\tau_{\text{CE}}(L, H, T) \approx A(T, L) \exp [\beta \Delta F_{\text{CE}}] , \quad (13)$$

where the prefactor $A(T, L)$ is nonuniversal. The dominant behavior of this approximate result agrees with other studies.⁸⁸⁻⁹⁰ The switching field H_{sw} was explicitly defined in Subsec. IIC as the absolute value of the field that corresponds to a specified waiting time τ for given L and T . An approximate form for H_{sw} , valid in the CE regime, is obtained by solving Eq. (13) with ΔF_{CE} given by Eq. (12) for $|H|$ at fixed τ , while ignoring the pre-exponential L dependence:

$$H_{\text{sw}}(L, \tau, T) \approx \begin{cases} 0 & \text{for } L \leq d^{\frac{1}{1-d}} L_{\text{ThSp}}(\tau) \\ \frac{[\Omega d^d / 2^d]^{\frac{1}{d-1}}}{2Lm_{\text{sp}}} \left(2\sigma - \frac{\ln(\tau/A)}{\beta L^{d-1}} \right) & \text{for } d^{\frac{1}{1-d}} L_{\text{ThSp}}(\tau) \leq L \leq L_{\text{ThSp}}(\tau) \end{cases} . \quad (14)$$

The second line in this equation represents a rapidly increasing function of L . Here

$$L_{\text{ThSp}}(\tau) = \left[d \frac{\ln(\tau/A)}{2\beta\sigma} \right]^{\frac{1}{d-1}} \quad (15)$$

is a value of L which can be shown to correspond to the system size at which the switching process crosses over into the *single-droplet* regime (see below), known as the “thermodynamic spinodal” (ThSp).^{81,82} The thermodynamic spinodal is the point at which the free energy of the critical droplet discussed in Subsec. III A above equals that of a slab. It corresponds to a first-order phase transition in the fixed-magnetization ensemble.^{87,91} Since the free energies of both these excitations are proportional to their interface areas, this corresponds to $d\Omega R_c^{d-1} \approx 2L^{d-1}$. The value of the switching field at the thermodynamic spinodal is therefore given by

$$H_{\text{ThSp}} \approx \frac{1}{2} \left(\frac{\Omega d}{2} \right)^{\frac{1}{d-1}} \frac{(d-1)\sigma}{[L_{\text{ThSp}}(\tau) - \ell]m_{\text{sp}}} , \quad (16)$$

where ℓ is a weakly temperature-dependent phenomenological parameter of order unity (see Table I), which is fitted to simulation data in order to compensate for finite-size effects.⁸ In the remainder of this paper we do not consider corrections of the type accounted for by ℓ , but we point out that without such corrections, the peak in the switching field found numerically for the small systems we can simulate is not in very good agreement with Eq. (16).

The *single-droplet* (SD) regime^{81,82} is the part of the L - H plane characterized by systems for which the first critical droplet to nucleate grows to the size of the system before a second critical droplet nucleates. The lifetime in the SD regime approximately equals the average time until the first droplet nucleates,

$$\tau_{\text{SD}} \approx t_{\text{nuc}} = (L^d I)^{-1} \propto L^{-d} \exp [\beta \Delta F_{\text{SD}}] . \quad (17)$$

Solving this equation with ΔF_{SD} given by Eq. (10) for $|H|$ at fixed τ , we obtain an approximate form for the switching field in the SD regime:

$$H_{\text{sw}}(L, \tau, T) \approx \frac{d-1}{2m_{\text{sp}}} \left[\frac{\beta\Omega\sigma^d}{\ln(\tau L^d/B)} \right]^{\frac{1}{d-1}} \text{ for } L > L_{\text{ThSp}}(\tau). \quad (18)$$

This is a monotonically decreasing function of L . Due to the neglect of prefactors in the derivations of Eqs. (14) and (18), these estimates for the switching field do not match perfectly at L_{ThSp} . One function of the adjustable parameter ℓ in Eq. (16) is to provide this matching.

Equations (14) and (18) show that the derivative of H_{sw} with respect to L at fixed τ is positive in the CE regime and negative in the SD regime. The crossover between these two regimes must therefore be associated with a maximum in the switching field. We emphasize that the presence of this peak is due *solely to a nonequilibrium crossover* and not to the effects of magnetostatic dipole-dipole interactions⁷ which can cause the equilibrium system to be composed of more than a single domain. This is in contrast to Eq. (2), which indicates that the switching field increases monotonically as long as the system is single-domain in equilibrium.

In both the CE regime and the SD regime, switching is abrupt, with a negligible amount of time spent in configurations with magnetizations significantly different from $\pm m_{\text{sp}}$, and switching is a Poisson process. This phenomenon, in which the entire system behaves as though it were a single magnetic moment, is known as superparamagnetism.^{2,3} As a consequence of the Poisson nature of the switching process, the standard deviation of the lifetime for an individual grain is approximately equal to the mean lifetime, τ . Because of the random nature of switching of these two regions of the L - H plane, they have been jointly called^{81,82} the “stochastic” region.

We can combine Eqs. (10), (12) and (16) (the latter with $\ell=0$) into the convenient form

$$\frac{\Delta F}{\Delta F_{\text{SD}}} = \begin{cases} d \left(\frac{|H|}{H_{\text{ThSp}}} \right)^{d-1} - (d-1) \left(\frac{|H|}{H_{\text{ThSp}}} \right)^d & \text{for } \frac{|H|}{H_{\text{ThSp}}} \leq 1 \\ 1 & \text{for } \frac{|H|}{H_{\text{ThSp}}} \geq 1 \end{cases}, \quad (19)$$

which is shown for $d=2$ in Fig. 2. By comparing Eqs. (9) and (16), we find that the argument in this equation has a transparent interpretation in terms of the relative sizes of the system and the critical droplet:

$$\frac{|H|}{H_{\text{ThSp}}} = \left(\frac{2^d}{\Omega d} \right)^{\frac{1}{d-1}} \frac{L}{2R_c}. \quad (20)$$

Although Eq. (19) is a monotonic function, it provides a clue to the existence of a peak in the switching field at the thermodynamic spinodal. For $|H| > H_{\text{ThSp}}$ (i.e., in the SD regime), the free-energy barrier for the nucleation of a droplet at a specified site becomes independent of the system size. This is basically because the shape of the droplet is independent of its radius. However, the system size still enters into the *lifetime* through the number of available nucleation sites, as shown in Eqs. (13) and (17). These entropic corrections to Eq. (19) and

their analogues for systems with nonperiodic boundary conditions are the main cause of the peak observed in the switching field. They are discussed in greater detail in Subsec. IV C below.

For fields that are not too strong, the radial growth velocity of a supercritical droplet is linear in $|H|$: $v = \nu|H|$.^{4,84,92–95} This leads to a competition between nucleation and growth. The *multidroplet* (MD) regime^{81,82} is the part of the L - H plane where the finite growth velocity allows other critical droplets to nucleate before the first critical droplet has grown to the size of the system. The crossover between the SD and MD regimes is known as the “dynamic spinodal” (DSp).^{81,82} A reasonable criterion to locate the DSp is that the nucleation time, $t_{\text{nuc}} = (L^d I)^{-1}$, and the time it takes a droplet to grow to a size comparable to L should be equal:^{4,91}

$$L^d I(T, H) = (2\Omega)^{-1/d} L^{-1} \nu |H|. \quad (21)$$

This yields the asymptotic relation^{4,82}

$$H_{\text{DSp}} \sim \frac{(d-1)}{2m_{\text{sp}}} \left[\frac{\beta\Omega\sigma^d}{(d+1)\ln L} \right]^{\frac{1}{d-1}}. \quad (22)$$

However, relatively large systems ($L \gtrsim 10^3$ – 10^4 for $d=2$) are required for the contribution described by Eq. (22) to be larger than the correction terms in the numerical solution of Eq. (21) (see Fig. 11 of Ref. 91).

In the MD regime the magnetization is a self-averaging quantity and develops deterministically with time according to “Avrami’s law:”^{24,82,96–98}

$$m(t) \approx 2m_{\text{sp}} \exp \left[- \left(\frac{t}{\tau_{\text{MD}}} \right)^{d+1} \right] - m_{\text{sp}}, \quad (23)$$

where

$$\tau_{\text{MD}} \approx \left[\frac{I\Omega v^d}{(d+1)\ln 2} \right]^{-\frac{1}{d+1}} \propto \exp \left[\frac{\beta\Delta F_{\text{SD}}}{d+1} \right] \quad (24)$$

gives the lifetime. The factor $d+1$ which occurs in Eqs. (23) and (24) is the space-time dimension of the system. Note that τ_{MD} is *independent* of L . Details of switching in the MD regime for systems with periodic boundary conditions are investigated elsewhere.^{84,99,100}

In the figures that show Monte Carlo results for the switching field versus L for various boundary conditions (Figs. 7, 9, 11, 12), the corresponding values for periodic boundary conditions are shown as dotted curves. The general shape expected from the above discussion — zero for small L , then a sharp rise, followed by a decline in the SD regime towards a plateau in the MD regime — is clearly observable.

IV. DROPLET THEORY FOR HETEROGENEOUS NUCLEATION

In this section we examine the free-energy barriers between the metastable and stable phases for two simple system geometries described in Subsec. II A: semiperiodic and circular

systems. In doing so, we restrict our theoretical considerations to two-dimensional systems, as we also do for our numerical study. However, the results can be generalized to $d=3$ in a straightforward manner. For simplicity, we also ignore the anisotropy of the interface tension. This is an excellent approximation for intermediate and high temperatures. In what follows, whenever we refer explicitly to quantities that correspond to homogeneous nucleation, such as cross-over fields or free-energy barriers, the special case $d=2$ and $\Omega=\pi$ is to be understood. We also maintain a nomenclature such that the terms “volume,” “area,” and “length” correspond to the two-dimensional equivalents of $(\text{length})^d$, $(\text{length})^{d-1}$, and $(\text{length})^1$, respectively.

As with systems with periodic boundary conditions, the dominant contribution to the lifetime is an exponential dependence on the free-energy barrier for a critical fluctuation centered at a particular site, as shown in Eqs. (13), (17), and (24). In Subsecs. IV A and IV B we obtain the corresponding free-energy barriers for semiperiodic and circular systems, respectively.

As was also discussed in Sec. III, the dominant behavior of the lifetime is modified by corrections involving the number of available nucleation sites and the applied field. We show in Subsec. IV C that these corrections can be viewed as entropy corrections to the free-energy barrier. The existence, size, and location of the peak in the switching field are determined by the manner in which these corrections depend on H and L .

The surface of a droplet of stable phase forming on the system boundary consists of two distinct parts. The first is an interior interface separating the droplet from the metastable background. This part of the droplet surface contributes a term to the total free energy of the system which is the product of its area and the interface tension, σ . The second is the part of the system boundary which is also part of the droplet. This exterior droplet surface contributes a term to the total free energy of the system which is the product of its area and the “boundary tension,” σ_Σ . This boundary tension expresses the *difference* in free energy per unit area between the system boundaries limiting the two different bulk phases.

For a two-dimensional system, we can exploit the exactly known free-energy density of the one-dimensional Ising model^{101,102} in an external field h ,

$$f_1(h) = -T \ln \left\{ e^{\beta J} \cosh[\beta h] + \sqrt{e^{-2\beta J} + e^{2\beta J} \sinh^2[\beta h]} \right\} , \quad (25)$$

to obtain a rough approximation for the boundary tension. Consider the chain of boundary spins. In addition to the external field H , they are also subject to interactions with the interior of the system, which we take into account in a mean-field approximation. This results in an additional effective field $\pm Jm_{\text{sp}}$, the sign of which depends on whether (+) or not (−) there is a droplet attached to the boundary of the system. In this way, one can get the contribution to the free energy from the boundary layer of spins as the free energy of a one-dimensional Ising system in an appropriate field. Then, an estimate of the boundary tension is given by

$$\sigma_\Sigma \approx [f_1(H + H_\Sigma + Jm_{\text{sp}}) - f_1(H + H_\Sigma - Jm_{\text{sp}})] - [f_1(H + Jm_{\text{sp}}) - f_1(H - Jm_{\text{sp}})] . \quad (26)$$

Here, the first and second terms represent the free-energy difference from the metastable phase due to the external boundary of the droplet with and without the applied surface field H_Σ , respectively. Note that $\sigma_\Sigma = 0$ when $H_\Sigma = 0$. This estimate is less accurate at

temperatures closer to the critical point, where the mean-field nature of the approximation causes σ_Σ to be overestimated.

Having estimated the boundary tension, we obtain the contact angle θ_Y of droplets forming at the system boundary from Young's relation:¹⁰³

$$\sigma \cos(\theta_Y) + \sigma_\Sigma = 0. \quad (27)$$

For $\sigma_\Sigma \geq \sigma$, Eq. (27) yields $\theta_Y = \pi$, corresponding to a completely “dry” boundary. For $\sigma_\Sigma = 0$, one has $\theta_Y = \pi/2$, and for $\sigma_\Sigma \leq -\sigma$, $\theta_Y = 0$ so that the stable phase completely “wets” the boundary. We emphasize that although σ_Σ depends on H , this dependence is practically negligible in the region of interest for this study. This is documented in Fig. 3, where we have plotted θ_Y as a function of H_Σ for two different values of H .

The determination of the droplet shape is directly related to studies of wetting.¹⁰⁴ Some readers may be aware that a wetting problem has been solved exactly by Abraham¹⁰⁵ for the two-dimensional Ising model, and that the droplet shape in that case is an ellipse,¹⁰⁶ not a circle. However, the systems Abraham studied were in zero field, and so this result and other zero-field studies¹⁰⁷ are not directly applicable to the current topic.

A. Semiperiodic Systems

As is the case for periodic boundary conditions, the decay rate is controlled by the nucleation process that has the lowest free-energy barrier. In addition to the bulk droplet and the slab connecting two sides with periodic boundary conditions, which were considered in Sec. III, we now also must consider a droplet nucleating on one of the open system boundaries [Fig. 4(a)] and a slab configuration formed by an interface parallel to the open boundaries [Fig. 4(b)]. Both these configurations in general give lower free-energy barriers than the ones previously considered. We therefore assume for the moment that nucleation on the boundary is preferred over nucleation in the bulk, and we neglect entropic terms which arise from translational invariance and other corrections. These issues are addressed in Subsec. IV C.

The free energy of a system composed of two “slabs” (sl) with magnetizations $\pm m_{\text{sp}}$ [Fig. 4(b)], corresponding to a system magnetization m , is

$$F_{\text{sl}}^\square(m) = L(\sigma + \sigma_\Sigma) + L^2|H|(m - m_{\text{sp}}). \quad (28)$$

The superscript \square is used to designate quantities specifically related to the nonperiodic boundaries of a semiperiodic system.

The droplets form preferentially on an open boundary with a contact angle θ_Y given by the Young equation, Eq. (27) [see Fig. 4(a)]. The magnetization of a system containing a single droplet of radius R is then given by

$$m = m_{\text{sp}} \left\{ 1 - 2\pi \left(\frac{R}{L} \right)^2 f(\theta_Y) \right\}, \quad (29)$$

where

$$f(\theta_Y) = \frac{2\theta_Y - \sin(2\theta_Y)}{2\pi}. \quad (30)$$

The droplet covers a boundary area equal to $2R \sin(\theta_Y)$ and has an interior interface of area $2R\theta_Y$. The difference from the free energy of a uniform metastable system is given by

$$\begin{aligned} F_d^\square(m) &= 2R \sin(\theta_Y) \sigma_\Sigma + 2R\theta_Y \sigma + L^2 |H| (m - m_{\text{sp}}) \\ &= 2\pi f(\theta_Y) \left(R\sigma - R^2 |H| m_{\text{sp}} \right) \end{aligned} \quad (31)$$

$$= \sigma L \sqrt{2\pi f(\theta_Y)} \sqrt{1 - \frac{m}{m_{\text{sp}}}} + L^2 |H| (m - m_{\text{sp}}) . \quad (32)$$

Equating Eqs. (28) and (32) yields the “droplet-slab” (ds) magnetization, at which the droplet and slab free energies are equal,

$$m_{\text{ds}}^\square = m_{\text{sp}} \left[1 - \frac{(1 - \cos \theta_Y)^2}{2\pi f(\theta_Y)} \right] . \quad (33)$$

Using the condition $(d/dm)F_d^\square(m)|_{m_{\text{ds}}^\square} = 0$, we find the thermodynamic spinodal (to leading order in $1/L$),

$$H_{\text{ThSp}}^\square \approx \frac{2f(\theta_Y)}{1 - \cos \theta_Y} \frac{\pi \sigma}{2L m_{\text{sp}}} = \frac{2f(\theta_Y)}{1 - \cos \theta_Y} H_{\text{ThSp}} . \quad (34)$$

Note that $H_{\text{ThSp}}^\square < H_{\text{ThSp}}$ for all $\theta_Y < \pi$.

To evaluate the free-energy barrier for $|H| \geq H_{\text{ThSp}}^\square$, we find the critical-droplet radius from Eq. (31) by setting $(d/dR)F_d^\square = 0$. This yields Eq. (9), just as for periodic boundary conditions. Thus the critical droplet radius is independent both of L and of θ_Y . The free-energy barrier is given by $F_d^\square(R_c)$:

$$\Delta F_{\text{SD}}^\square = f(\theta_Y) \frac{\pi \sigma^2}{2|H| m_{\text{sp}}} = f(\theta_Y) \Delta F_{\text{SD}} . \quad (35)$$

Note that $\Delta F_{\text{SD}}^\square < \Delta F_{\text{SD}}$ for all $\theta_Y < \pi$. For $|H| \leq H_{\text{ThSp}}^\square$, the free-energy barrier is just $F_{\text{sl}}^\square(m_{\text{ds}}^\square)$:

$$\Delta F_{\text{CE}}^\square = L\sigma(1 - \cos \theta_Y) - L^2 |H| m_{\text{sp}} \frac{(1 - \cos \theta_Y)^2}{2\pi f(\theta_Y)} . \quad (36)$$

It is worth pointing out that the above results for the special case of $\theta_Y = \pi$ (i.e., a completely “dry” boundary) are identical with the results for periodic boundary conditions with $d=2$ and $\Omega=\pi$. In particular, Eq. (31) corresponds to Eq. (8), Eq. (34) corresponds to Eq. (16), Eq. (35) corresponds to Eq. (10), and Eq. (36) corresponds to Eq. (12).

Just as for periodic boundary conditions, we can combine Eqs. (34), (35) and (36) to obtain

$$\frac{\Delta F^\square}{\Delta F_{\text{SD}}^\square} = \begin{cases} 2 \left(\frac{|H|}{H_{\text{ThSp}}^\square} \right) - \left(\frac{|H|}{H_{\text{ThSp}}^\square} \right)^2 & \text{for } \frac{|H|}{H_{\text{ThSp}}^\square} \leq 1 \\ 1 & \text{for } \frac{|H|}{H_{\text{ThSp}}^\square} \geq 1 \end{cases} , \quad (37)$$

which is the equivalent of Eq. (19) for $d=2$ and with the θ_Y dependent H_{ThSp}^\square instead of H_{ThSp} . This relation is illustrated in Fig. 2. As in Eq. (19), the argument has a simple interpretation in terms of the relative sizes of the system and the critical droplet:

$$\frac{|H|}{H_{\text{ThSp}}^\square} = \frac{1 - \cos \theta_Y}{\pi f(\theta_Y)} \frac{L}{2R_c}. \quad (38)$$

B. Circular Systems

Consider a circular droplet growing at the boundary of a circular system with a wetting angle of θ , illustrated as θ_Y in Fig. 5. If the droplet has radius R , then it subtends an arc of the particle boundary corresponding to an angle 2ϕ , where ϕ is given by

$$\phi\left(\frac{L}{2R}, \theta\right) = \text{ARCTAN}\left(\frac{L}{2R} + \cos(\theta), \sin(\theta)\right). \quad (39)$$

The two-argument function $\text{ARCTAN}(x, y)$ is the angle defined by¹⁰⁸

$$\cos(\text{ARCTAN}(x, y)) = \frac{x}{\sqrt{x^2 + y^2}}, \quad (40a)$$

$$\sin(\text{ARCTAN}(x, y)) = \frac{y}{\sqrt{x^2 + y^2}}, \quad (40b)$$

and

$$0 \leq \text{ARCTAN}(x, y) < 2\pi. \quad (40c)$$

To simplify the notation, we omit the arguments of the function ϕ in what follows. The volume of the droplet can be expressed as

$$V = \frac{L^2\phi}{4} + (\theta - \phi)R^2 - \frac{LR \sin(\theta)}{2}, \quad (41)$$

and the total free energy is given by

$$\mathcal{F}(R, \theta) = L\phi\sigma_\Sigma + 2R\sigma(\theta - \phi) - 2|H|m_{\text{sp}}V. \quad (42)$$

In order to obtain the wetting angle θ we minimize \mathcal{F} while holding V constant, so that

$$\frac{\partial \mathcal{F}}{\partial R} \frac{\partial V}{\partial \theta} - \frac{\partial \mathcal{F}}{\partial \theta} \frac{\partial V}{\partial R} = 0. \quad (43)$$

After factorization, this condition reads

$$\frac{[\sigma_\Sigma + \sigma \cos(\theta)] \left[(2R + L \cos(\theta))(\phi - \theta) + L \sin(\theta) \right] [4LR^2]}{L^2 + 4R^2 + 4RL \cos(\theta)} = 0. \quad (44)$$

It is clear that among its solutions, only the solution of the first factor in the numerator, corresponding to Young's relation, i.e., $\theta = \theta_Y$, is acceptable. This is because that is the only solution which depends on σ . Using this we find the free energy to be given by

$$\begin{aligned} F^\odot(R) &= \mathcal{F}(R, \theta_Y) \\ &= -L\phi\sigma \cos(\theta_Y) + 2R\sigma(\theta_Y - \phi) - 2|H|m_{\text{sp}}V. \end{aligned} \quad (45)$$

The superscript \odot is used to designate quantities specifically related to the boundary of a circular system.

Note that, in contrast to systems with periodic boundary conditions in at least one direction, there is no slab solution for circular systems. However, the droplet free energy, $F^\odot(R)$, depends quite differently on R and L in the two limits, $L/2R \rightarrow 0$ and $L/2R \rightarrow \infty$. In the former case, which corresponds to a droplet with an almost flat inner interface, it is easy to see from Eq. (39) that $\phi \rightarrow \theta_Y$. In this limit, $F^\odot(R)$ is therefore independent of R and linear in L . In the latter case, which corresponds to a droplet which is so small that the system boundary appears flat in comparison, we expand ϕ in powers of $2R/L$:

$$\phi \approx \frac{2R}{L} \sin(\theta) - \left(\frac{2R}{L}\right)^2 \cos(\theta) \sin(\theta) + \dots \quad (46)$$

It is easy to see that in the limit $L/2R \rightarrow \infty$, Eq. (45) with V given by Eq. (41) is identical to Eq. (31) for semiperiodic systems, as expected. Thus, in this limit the free energy is linear in R and independent of L .

A simple calculation shows that the critical radius R_c is not affected by the boundary conditions and is again given by Eq. (9). As a result, we obtain the free-energy barrier

$$\Delta F^\odot = F^\odot(R_c). \quad (47)$$

Since $\lim_{L/2R_c \rightarrow \infty} \Delta F^\odot = \Delta F_{\text{SD}}^\square$, it is reasonable to try to express the crossover of ΔF^\odot with $L/2R_c$ in a scaling form similar to Eqs. (19) and (37). Specifically, we get

$$\frac{\Delta F^\odot}{\Delta F_{\text{SD}}^\square} = \frac{\theta_Y - \phi(x, \theta_Y) [1 + x^2 + 2x \cos(\theta_Y)] + x \sin(\theta_Y)}{\pi f(\theta_Y)}, \quad (48a)$$

where

$$x \equiv \frac{L}{2R_c} = \frac{\pi}{2} \frac{|H|}{H_{\text{ThSp}}^\square} = \frac{1 - \cos \theta_Y}{\pi f(\theta_Y)} \frac{|H|}{H_{\text{ThSp}}^\square}, \quad (48b)$$

and H_{ThSp}^\square is given by Eq. (34). Note that x does *not* depend on θ_Y ; it simply expresses the system size in units of the critical droplet size. Equation (48) thus shows that the free-energy barrier for circular systems, when normalized by the free-energy barrier for a semiperiodic system with the same value of θ_Y , is a function of the field only through $|H|/H_{\text{ThSp}}^\square$. However, the absence of a slab solution implies that there is no sharply defined thermodynamic spinodal for circular systems. The crossover is therefore much more gradual than in systems with periodic boundaries in at least one direction. Figure 2 shows $\Delta F^\odot/\Delta F_{\text{SD}}^\square$ for two different values of θ_Y .

C. Entropy Effects Due to Translational Invariance

As mentioned briefly in Subsecs. III B, IV A, and IV B above, the scaling relations for the free-energy barriers [Eqs. (19), (37), and (48) for periodic, semiperiodic and circular systems, respectively], if interpreted as scaling relations for the logarithm of the metastable lifetimes, do *not* predict a peak in the switching field when considered as functions of the system size at constant waiting time. This peak, the dependence of which on the boundary conditions is the main topic of the present paper, is chiefly the result of entropic terms that correspond to the number of available nucleation sites. When these terms are considered as corrections to the free-energy barriers of the droplets discussed above, they lead to corrections that are logarithmic in L . They decrease the free-energy barrier as the system size increases, and, as a consequence, the switching field is a decreasing function of the system size. We note that these entropy effects are analogous to the translational corrections to the nucleation rates in fluids, previously introduced by Lothe and Pound.¹⁰⁹ This argument applies only in the SD regime, and the switching-field maximum can be observed only if the entropic terms start to be discernible before the crossover into the MD regime sets in.

Other terms in the free-energy barrier that are logarithmic in the applied field arise from power-law prefactors in the nucleation rate, such as the one explicitly included in Eq. (11). These terms are identical for droplets nucleating in the bulk and droplets nucleating on the system boundary, at least within the approximations described in this paper. The growth times also need to be considered. These yield terms proportional to $\ln(L/|H|)$, as well as constant terms. Only the constant terms are different for bulk and surface droplets. Consequently, none of these terms are important in the lowest-order approximation. We shall find it more convenient to consider the terms arising from power-law prefactors in the nucleation rates part of the free-energy barriers, but to treat the growth time separately.

We begin with a system with semiperiodic boundary conditions for which switching occurs through nucleation at the system boundary, which is of area $2L$. Then Eqs. (11), (17), and (35) yield for the lifetime:¹¹⁰

$$T \ln t_{\text{nuc}}^{\square} \equiv \widehat{\Delta F}_{\text{SD}}^{\square} = f(\theta_Y) \frac{\pi \sigma^2}{2|H|m_{\text{sp}}} - T \ln(2L) - TK \ln |H|. \quad (49)$$

Here and henceforth, the notation $\widehat{\Delta F}$ is taken to mean a free-energy barrier for a droplet in which the entropy-related corrections (or, in other words, the “effect of the number of nucleation sites”) as well as terms proportional to $K \ln |H|$ are included. Similarly, the free-energy barrier for nucleating a single droplet in the bulk is obtained from Eqs. (10), (11), and (17):

$$T \ln t_{\text{nuc}} \equiv \widehat{\Delta F}_{\text{SD}} = \frac{\pi \sigma^2}{2|H|m_{\text{sp}}} - T \ln(L^2) - TK \ln |H|. \quad (50)$$

Nucleation in the bulk will be the dominant decay mode only if there exists a range of L and H such that $\widehat{\Delta F}_{\text{SD}} < \widehat{\Delta F}_{\text{SD}}^{\square}$. The crossover point in the L - H plane can therefore be found as a function of the nucleation time by solving Eqs. (49) and (50) together. For sufficiently weak fields we can ignore the $\ln|H|$ terms. If we further make the assumption that the waiting time τ approximately equals the nucleation time, which is valid for single-droplet decay, we obtain:

$$H_{\times}(\tau) \approx \frac{\beta\pi\sigma^2 [2f(\theta_Y) - 1]}{2m_{\text{sp}} \ln(4\tau)} \quad (51a)$$

and

$$L_{\times}(\tau) \approx \left(2\tau^{[1-f(\theta_Y)]}\right)^{\frac{1}{2f(\theta_Y)-1}}. \quad (51b)$$

These solutions are physically acceptable only if

$$\frac{1}{2} < f(\theta_Y) \leq 1, \quad (52)$$

which means that there can be a transition from boundary nucleation to bulk nucleation only if

$$\frac{\pi}{2} < \theta_Y \leq \pi. \quad (53)$$

Eq. (51b) gives an estimate of the system size above which bulk nucleation dominates over nucleation at the boundary for a given waiting time. On the other hand, in systems smaller than $L_{\times}(\tau)$, the majority of the critical droplets will nucleate at the boundary. We emphasize that the crossover between these two regimes is not sharp, but we have observed both regimes in Monte Carlo simulations, with a crossover in semiquantitative agreement with Eq. (51).

The above arguments indicate that for $\theta_Y > \pi/2$, there exist circumstances in which the first droplet to nucleate forms in the bulk, rather than on the boundary. However, one may still ask whether the transition from boundary-dominated nucleation to bulk-dominated nucleation takes place in the SD regime or in the MD regime. In analogy with Eq. (21), the dynamic spinodal for semiperiodic systems may be defined by the equality of the nucleation time and the growth time:

$$L \exp\left(-\beta\widehat{\Delta F}_{\text{SD}}^{\square}\right) = \pi^{-1/2}L^{-1}\nu|H|, \quad (54)$$

with the asymptotic solution

$$H_{\text{DSp}}^{\square} \sim \frac{1}{2}f(\theta_Y)\frac{\beta\pi\sigma^2}{2m_{\text{sp}} \ln L} = \frac{3}{2}f(\theta_Y)H_{\text{DSp}}. \quad (55)$$

In order for bulk nucleation to dominate surface nucleation in the SD regime, we must have $H_{\text{DSp}}^{\square} \gtrsim H_{\times}$, which yields

$$f(\theta_Y) \geq \frac{2}{3}. \quad (56)$$

We designate as θ_{bulk} the value of θ_Y which satisfies Eq. (56) as an equality, and we find numerically that $\theta_{\text{bulk}} \approx 0.585\pi$.

In summary, the changes in the decay mode from boundary-dominated single-droplet decay with increasing L proceed differently, depending on the value of θ_Y .

- For $\theta_Y \lesssim \pi/2$, nucleation at the boundary is always more likely than nucleation in the bulk. As L increases, the system crosses the boundary dynamic spinodal, H_{DSp}^{\square} , and the decay changes from the boundary-dominated single-droplet mode to the boundary-dominated multidroplet mode. Bulk nucleation does not occur for any value of L .

- For $\pi/2 \lesssim \theta_Y \lesssim \theta_{\text{bulk}}$, multidroplet nucleation at the boundary becomes dominant at a value of $L < L_\times$. As L is increased further, bulk multidroplet nucleation becomes the dominant decay mode.
- For $\theta_{\text{bulk}} \lesssim \theta_Y \lesssim \pi$, bulk single-droplet nucleation dominates for $L \gtrsim L_\times$. For sufficiently large L the system crosses the bulk dynamic spinodal, H_{Dsp} , and the bulk multidroplet decay mode becomes dominant.
- For $\theta_Y = \pi$, bulk nucleation is dominant for all L .

The effects of the entropic terms on the switching field are shown in Fig. 6.

Although here we only explicitly consider the effects of translational invariance for semiperiodic systems, at high temperatures we expect no significant difference for systems with fully open boundaries, such as circles. At low temperatures, the anisotropy of the interface tension may cause some nucleation sites to be preferred on the boundaries of circles, thus diminishing the translational invariance.

V. MONTE CARLO SIMULATIONS

The theoretical results of the previous section deal most carefully with those effects which should be dominant in the limit of long waiting time, where the switching field is small and the droplets are large. In this section we use Monte Carlo simulations to demonstrate that the results of the previous section hold quite well even when the lifetime is not extremely long, so that the switching field is rather large and the droplets rather small.

A. Semiperiodic Systems

In Fig. 7 we present the switching fields for semiperiodic systems as functions of the system size for $T = 1.3J \approx 0.57T_c$ and for different values of the surface field H_Σ . Panels (a) and (b) of the figure correspond to the waiting times $\tau = 1000$ and 30000 Monte Carlo Steps per Spin (MCSS), respectively. In both cases we see similar behavior, depending on the value of H_Σ . For large H_Σ , a semiperiodic system behaves very much like a periodic one. The peak of the switching field is pronounced because there is a well distinguished region of system sizes in which single-droplet nucleation is dominant. For $H_\Sigma = 1.0$ the critical droplet typically nucleates in the bulk even in small systems, whereas for $H_\Sigma = 0.5$ it usually appears at the boundary. As the system size increases, nucleation in the bulk becomes the more important process in both cases, and the switching fields gradually approach those measured for the periodic system. For $H_\Sigma = 0.5$, this corresponds to the crossover from single-droplet nucleation at the boundary to single-droplet nucleation in the bulk, as described for $\theta_{\text{bulk}} \lesssim \theta_Y \lesssim \pi$ in Subsection IV C. This switching-field behavior also qualitatively corresponds to the expectation based on our estimates of the contact angles of the droplets. From Fig. 3 it is seen that for $H_\Sigma = 1.0$ the droplets do not wet the boundary, and that is why the semiperiodic systems behave essentially in the same way as periodic ones. For $H_\Sigma = 0.5$, we expect the contact angle at this temperature to be about 0.7π and, therefore, boundary nucleation should prevail in small systems, as is also observed.

However, the crossover system size L_{\times} predicted in Eq. (51b) for these particular conditions is somewhat too small. We attribute this to the fact that the formula is expected to be valid for large systems, while our simulations are carried out for rather small L . Observations of configuration snapshots during our simulations reveal that the crossover to bulk nucleation takes place at larger L , between $L = 20$ and $L = 100$, without exhibiting a sharp crossover. In Fig. 8 we show snapshots of typical configurations with supercritical droplets in systems with $L = 10$ and $L = 50$.

The switching behavior is rather different with zero applied surface fields, $H_{\Sigma} = 0.0$. In that case, the droplets have a contact angle equal to $\pi/2$, which corresponds to a free boundary. Consequently, nucleation at the boundary is greatly preferred over nucleation in the bulk. As L increases, the system crosses over from the single-droplet regime into the multidroplet regime, but with the droplets still nucleating at the boundary. The maximum of the switching field in the vicinity of the thermodynamic spinodal is still visible, but the peak is much less pronounced than in cases with strong surface fields. This is due to two effects. First, the short waiting time makes the SD regime rather narrow, so that entropic terms in the free-energy barriers do not have much chance to assert themselves. Second, the entropic terms for nucleation at the boundary are smaller than those corresponding to nucleation in the bulk [see Eqs. (49) and (50)] and so is their effect on the switching field. This observation is in agreement with Eq. (53), which indicates that the crossover system size L_{\times} should diverge for $\theta_Y = \pi/2$. For very large systems, the switching field increases and approaches the one measured for periodic systems. This is because the growth time becomes comparable to the nucleation time. The decay process then proceeds as follows. First, many droplets nucleate at the open boundaries and coalesce to create slabs of stable phase. Next, these slabs grow into the bulk until the magnetization is reversed. In this regime, to keep the lifetime constant while increasing L , one has to increase the field in order to compensate for the longer distance the growing interfaces have to travel.

Finally, in Fig. 7 we see that Monte Carlo evaluations of the switching fields are in agreement with the theory discussed above. This makes these curves appear very similar to each other, even though the waiting times differ by a factor of thirty. Thus, we expect the theory to hold for all large values of τ and to produce visually similar curves. This is important because a comparison of typical atomic time scales with typical experimental time scales leads us to believe that values of τ relevant to experiments must be large numbers — much larger than can be simulated using Monte Carlo. In the next subsection, we will make theoretical extrapolations to this regime of large τ for circular systems, which are more physically relevant than semiperiodic systems.

Comparing the shapes of the switching-field plots in Fig. 7 with the theoretical predictions presented in Fig. 6, one can see that nucleation theory reflects the observed switching dynamics very well.

B. Circular Systems

Next we proceed with circular systems. Figs. 9(a) and (b) show the switching fields measured under the same conditions as those for the semiperiodic ones discussed above. One can see from the plots, as well as from simulation snapshots, that the behavior of

the circular systems is rather similar to that of semiperiodic lattices. There are two main differences.

The first difference from the semiperiodic systems is that the switching field peaks are less pronounced. This effect is easy to understand when we compare the behavior of the free-energy barriers without entropy terms in Fig. 2. Since there is no sharp crossover between a coexistence regime and a single-droplet regime in circular systems, the maxima in the switching fields are shifted to larger system sizes and become flatter. In a system with weak boundary fields, like the one shown in Fig. 9(a), this can lead to the complete disappearance of the maximum. Instead, one observes a plateau which is eventually followed by an increase of the switching field at the crossover to the multidroplet regime. Although this is a typical situation, one can observe a weak maximum of the switching field even in circular systems with free boundaries, even without applied surface fields. This is demonstrated in Fig. 9(b) for $H_{\Sigma} = 0.0$. Though hardly discernible on the scale of the figure, there is a clear maximum in the switching field. The whole data set shown belongs to the single-droplet regime, and the decrease of the switching field would continue if we were to include even larger systems. Thus, the existence of the maximum of the switching field depends on the specific conditions under which the measurement is carried out.

Second, one can observe small oscillations in the switching fields as functions of L for small systems. This is because in small systems the lattice structure in the vicinity of the boundary can influence the free-energy barriers (these types of corrections go beyond the theory presented in the previous section), and the interplay between the bulk and the boundary may depend significantly on the size of the system if it is small enough.

C. Octagonal Systems

The theory presented in Section IV treats the effects of the boundaries in a phenomenological way, mimicking them by an effective interface tension assigned to that surface of the droplet which is also part of the system edge. Naturally, the structure of the lattice and interactions near the boundary can also influence the dynamics of the droplet surface fluctuations. These effects are not captured by our simple theory and may be expected to produce pre-exponential corrections to the metastable lifetime. To see whether our approach can really describe the essence of the physics in systems with different boundary structures, we have simulated the magnetization switching in octagonal systems with their boundaries modified as described in Subsection II A.

For small systems on a square lattice, the best approximation to a circle is the same as the best approximation to an octagon. In order to observe a difference in shape, we need $L > 20$. For $T = 0.9T_c$ and $\tau = 2000$ MCSS, the switching field is nonzero only for $L > 20$ (see Fig. 10). Even so, Fig. 10 shows that there is little difference between the switching fields for octagonal systems (shown in Fig. 1) and for circular systems (which have no special provision to ensure that boundary sites all have the same number of neighbors).

Naturally, the difference between the octagonal and circular lattices becomes more discernible at lower temperatures where the interfacial tension becomes anisotropic, and the role of the lattice irregularities at the boundary is also more important since the flipping probabilities of spins with different neighborhoods are further separated. However, our observations indicate two things:

- For the weak fields at which a peak in H_{sw} vs. L might be expected, the theory developed in the previous section for circular systems appears to be applicable to octagonal systems as well for the range of fields and waiting times employed in this study.
- Geometric features much smaller than the critical droplet radius, such as omitted boundary bonds, are much less important than geometric features on the scale of the critical droplet radius, such as corners.

Figure 11 shows how boundary fields change the qualitative dependence of the switching field H_{sw} on the system size L of an octagonal system. For $H_{\Sigma} = 0$, which corresponds to open boundary conditions without any modifications (i.e., $J_{\Sigma} = 0$), we did not observe a peak in the switching field for these specific temperatures and waiting times. At both temperatures shown, the switching field monotonically increases with the system size and approaches its asymptotic value for very large systems. The absence of the peak is easy to understand in terms of the theory developed in the previous section: The crossover to the multidroplet regime, in which the switching field should be fairly constant, sets in before the decrease due to entropic terms can become discernible. As H_{Σ} is increased, the peak structure gradually develops and the switching field behavior becomes similar to that of a periodic system. One can see that for large enough systems the switching field is the same as that for periodic systems. The system size at which this occurs corresponds to the crossover from boundary nucleation to bulk nucleation as described in Subsection IV C. This behavior is clearly seen for a strong boundary field, $H_{\Sigma} = 1.0$, at both temperatures. At $T = 0.8T_c$, the droplets then practically do not wet the boundary, and even very small systems behave very much like periodic systems. For $T = 1.3J$ the contact angle corresponding to $H_{\Sigma} = 1.0$ is less than π and larger than $\pi/2$. In this case Eq. (26) is not expected to provide a good approximation for the boundary tension σ_{Σ} and for the resulting contact angle θ_Y , because the boundary of the octagon with modified coordinations does not have the topology of a chain. Compared to circular systems, octagons are slightly less sensitive to the surface fields, which may be caused by the fact that not all their boundary spins interact directly.

Similar effects, namely the disappearance of the switching-field peak, can also be observed for lattices which have modified spin-spin interactions close to their boundaries. This is shown in Fig. 12. In the switching-field behavior, these systems are more similar to the samples with $H_{\Sigma} = 0$ than to samples with nonzero boundary fields. In addition to increasing the switching field, some irregularity is observed in the plot of H_{sw} vs. L . This is apparently due to the fact that for small systems, the ratio of the length of a (10) face to the length of a (11) face depends nonmonotonically on L . This is a consequence of the fact that an ideal octagon cannot be constructed on a square lattice. The irregularity also indicates that there is still a difference between the (10) and (11) faces, in spite of the fact that boundary spins on both faces have two nearest neighbors.

For large systems, $J_{\Sigma} > 0$ can be expected to yield similar results to $H_{\Sigma} > 0$. This can most easily be seen for large systems with $J_{\Sigma} \rightarrow \infty$. With a single-spin-flip dynamic, it is *impossible* for either surface spins or the outermost layer of bulk spins to flip (see Fig. 1) in the limit $J_{\Sigma} \rightarrow \infty$. The coupling between these frozen spins and the unfrozen bulk spins makes the system very similar to an octagon of size $L - 4$ with $H_{\Sigma} = 1$ on the (10) faces and with $H_{\Sigma} = 2$ on the (11) faces. Since the frozen spins still count towards the value

of m [Eq. (4)], the switching field will in this case be greatly increased for small systems. However, for larger systems, the behavior of the switching field is quite similar to other types of systems studied here. This is an expression of the fact that it is only the affinity of the boundary to the stable phase which is important for the switching behavior rather than the details of interactions in the vicinity of the system boundary.

Thus, in spite of some quantitative differences between octagonal and circular systems, the basic behavior is very much the same, and we can conclude that the main features are well described by the nucleation theory from the previous section. On the other hand, it is seen that to achieve an accurate quantitative agreement between the theory and the simulation results, the theory would be required to include the dependence of the nucleation dynamics in the vicinity of lattice boundaries with different structures.

VI. CONCLUSIONS

We have studied the magnetization reversal dynamics in kinetic Ising systems with various kinds of boundaries. Our study emphasizes the stochastic regime of the space of magnetic fields and system sizes, in which the magnetization reversal is triggered by a single critical fluctuation. As expected, even minor modifications of the boundary conditions can lead to pronounced changes in the measured values of the metastable lifetime and switching fields. However, our simulations show that in spite of the quantitative differences, all the systems studied in this work are essentially described by the droplet nucleation theory outlined in Section IV. This theory allows us to understand in detail the behavior of the switching fields as functions of the temperature, system size, and waiting time. In particular, it can predict under which conditions it is possible to observe a maximum (peak) in the switching field as a function of L , and the extent of the single-droplet nucleation regime in the presence of boundaries.

Magnetization switching in systems with boundaries displays a rich variety of nucleation and growth behaviors. Roughly speaking, the single-droplet and multidroplet regimes known from periodic systems come in two flavors in systems with boundaries. In each regime, the dominant nucleation sites can be located either close to the boundary or in the bulk of the system. Depending on the waiting time and the wetting angle, one can observe crossovers between these regimes, although the crossover regions can be rather wide.

Qualitatively, the switching field behavior in the stochastic regime of a system with a boundary is similar to that in a periodic system if the contact angle of the droplets is larger than a right angle. If the contact angle is about $\pi/2$, the maximum in the switching field is in general suppressed and sometimes disappears completely.

The structure of the system boundary can have a pronounced effect on the lifetime. Nevertheless, if the critical size of a droplet is larger than the irregularities at the boundary, then the switching field does not depend strongly on these details. The main contribution to the lifetime depends only on the attractive or repulsive influence of the boundary towards large droplets. However, for an accurate quantitative description of the switching dynamics, a complete understanding of the fluctuation dynamics of droplets close to the boundary may be required.

Finally, we stress again that in this model the existence of a maximum in the switching field as a function of the system size has nothing to do with multidomain particles. The

systems studied here are single domain, and the switching field peaks are purely dynamic phenomena due to entropic effects and to a crossover between a regime in which the free energy of the critical fluctuation depends primarily on the applied field, and one in which it is determined by the system size. In systems with periodic boundary conditions this crossover is quite sharp and associated with a transition between well-defined single-droplet and coexistence regimes. Systems without periodic boundary conditions do not have a well-defined coexistence regime. However, the crossover behavior remains easily observable.

Although the kinetic Ising model is certainly too simplified for quantitative agreement with experimental observations to be expected, it is tempting to ask to what extent our theory is capable of yielding results in a physically sensible range. For this purpose, we consider a hypothetical ferromagnetic monolayer which would correspond to our simulations of circular systems. We take its lattice constant as 0.3 nm, and its Curie temperature as 375K. This implies a model exchange-interaction constant of $J = 1.42 \times 10^{-2}$ eV (compare with the exchange constant 1.19×10^{-2} eV of iron¹¹¹). With each atom we associate a magnetic moment of one Bohr magneton, $\mu_B = 5.788 \times 10^{-5}$ eV T⁻¹. This would correspond to $S = 1/2$ and a gyromagnetic ratio $g = 2$. Another necessary input is the relation between Monte Carlo time and real time, which is determined mainly by phonon frequencies. Thus, 10^{12} MCSS could roughly correspond to a physical time interval on the order of seconds. The prefactor which connects the exponential of the free-energy barrier in nucleation theory with the metastable lifetime is assumed to be of order unity. The switching fields for a waiting time of 10^{13} MCSS, calculated for the above parameters at room temperature, comparable to $0.8T_c$ (at which temperature the interface tension of the Ising model is $\sigma = 0.7459J$), are shown in Fig. 13.

The simple insertion of physical parameters into our theoretical formulae, discussed in the previous paragraph, predicts switching fields that depend on the system size in a way very similar to experimental observations. However, the predicted switching fields are about one order of magnitude stronger than typical switching fields for nanoscale ferromagnetic systems. Also, the calculated switching fields grow with decreasing temperature or, equivalently, the calculated waiting times for realistic switching fields are unphysically long at lower temperatures. Nevertheless, keeping in mind the extreme simplicity of the model, we find this comparison very promising. Allowing for finite anisotropy of the model and including effects of disorder will decrease the switching fields significantly. Such investigations are already in progress.⁹ The theoretical and numerical results of this study raise the exciting possibility that the convergence of more realistic microscopic spin models and further experimental studies of the statistical switching behavior of well-characterized single-domain samples soon may provide quantitative, as well as qualitative, agreement between theoretical and experimental results.

ACKNOWLEDGMENTS

The authors wish to thank S. von Molnár for useful discussions. At various times during this project, H. L. R. and P. A. R. enjoyed hospitality and support at the Risø National Laboratory and at Kyoto University, respectively. P. A. R.'s visit to Kyoto University was supported by the Center for Global Partnership Science Fellowship Program through U. S. National Science Foundation Grant No. INT-9512679. This research was supported

in part by the Florida State University Center for Materials Research and Technology, by the FSU Supercomputer Computations Research Institute, which is partially funded by the U. S. Department of Energy through Contract No. DE-FC05-85ER25000, by the U. S. National Science Foundation through Grants No. DMR-9520325 and DMR-9315969, and by the Inoue Foundation for Science. Computing resources at the National Energy Research Supercomputer Center were made available by the U. S. Department of Energy.

REFERENCES

- * Current address at The University of Tokyo. Electronic address: richards@shpd.phys.s.u-tokyo.ac.jp
- † Permanent address: Institute of Physics, SAS, Dúbravská cesta 9, 842 28 Bratislava, Slovakia. Electronic address: kolesik@scri.fsu.edu
- & Electronic address: p.a.lindgard@risoe.dk
- ‡ Current and permanent address at Florida State University. Electronic address: rikvold@scri.fsu.edu
- § Electronic address: novotny@scri.fsu.edu
- ¹ E. F. Kneller and F. E. Luborsky, *J. Appl. Phys.* **34**, 656 (1963).
- ² I. S. Jacobs and C. P. Bean, in *Magnetism*, edited by G. T. Rado and H. Suhl (Academic, New York, 1963), Vol. 3, p. 271.
- ³ C. P. Bean and J. D. Livingston, *J. Appl. Phys.* **30**, 120S (1959).
- ⁴ H. L. Richards, S. W. Sides, M. A. Novotny, and P. A. Rikvold, *J. Magn. Magn. Mater.* **150**, 37 (1995).
- ⁵ H. L. Richards, S. W. Sides, M. A. Novotny, and P. A. Rikvold, in *Physical Phenomena at High Magnetic Fields*, edited by Z. Fisk, L. Gorkov, D. Meltzer and R. Scrieffer, (World Scientific, Singapore, 1995), p. 386.
- ⁶ H. L. Richards, S. W. Sides, M. A. Novotny, and P. A. Rikvold, *J. Appl. Phys.* **79**, 5749 (1996).
- ⁷ H. L. Richards, M. A. Novotny, and P. A. Rikvold, *Phys. Rev. B* **54**, 4113 (1996).
- ⁸ H. L. Richards, Ph.D. thesis, Florida State University, 1996.
- ⁹ M. Kolesik, H. L. Richards, M. A. Novotny, P. A. Rikvold and P.-A. Lindgård, *J. Appl. Phys.*, submitted.
- ¹⁰ L. Néel, *Ann. Géophys.* **5**, 99 (1949).
- ¹¹ W. F. Brown, *J. Appl. Phys.* **30**, 130S (1959); *Phys. Rev.* **130**, 1677 (1963).
- ¹² J. H. Van't Hoff, *Etudes de Dynamiques Chimiques*, F. Muller and Co., Amsterdam, 1884; S. Arrhenius, *Z. Phys. Chem. (Leipzig)* **4**, 266 (1889).
- ¹³ W. F. Brown, *Micromagnetics* (Wiley, New York, 1963); S. Shtrikman and D. Treves, in *Magnetism*, edited by G. T. Rado and H. Suhl, (Academic, New York, 1963) volume 3, page 395.
- ¹⁴ A. Aharoni, *Introduction to the theory of ferromagnetism* (Clarendon Press, Oxford, 1996).
- ¹⁵ A. Lyberatos, D. V. Berkov, and R. W. Chantrell, *J. Phys.: Cond. Matter* **5**, 8911 (1993); A. Lyberatos and R. W. Chantrell, *J. Phys. D: Appl. Phys.* **29**, 2332 (1996).
- ¹⁶ See C. L. Wang and S. R. P. Smith, *J. Phys.: Condens. Matter* **8**, 4813 (1996), and references therein.
- ¹⁷ R. D. Kirby, J. X. Shen, R. J. Hardy, and D. J. Sellmyer, *Phys. Rev. B* **49**, 10810 (1994).
- ¹⁸ R. Mélin, cond-mat/9603026, to appear in *J. Magn. Magn. Mater.*
- ¹⁹ P. A. Serena and N. García, in *Quantum Tunneling of Magnetization – QTM'94*, edited by L. Gunther and B. Barbara (Kluwer, Dordrecht, 1995), p. 107.
- ²⁰ D. García-Pablos, P. García-Mochales, N. García, and P. A. Serena, *J. Appl. Phys.* **79**, 6019 (1996).
- ²¹ U. Nowak and A. Hucht, *J. Appl. Phys.* **76**, (1994).
- ²² S. T. Chui and D.-C. Tian, *J. Appl. Phys.* **78**, 3965 (1995).

- ²³ These droplets are sometimes called domains, but we reserve the term “domain” for an *equilibrium* region of uniform magnetization, the size of which is determined by the magnetostatic dipole-dipole interaction and by the exchange interaction.
- ²⁴ P. A. Rikvold and B. M. Gorman, in *Annual Reviews of Computational Physics I*, edited by D. Stauffer (World Scientific, Singapore, 1994), p. 149.
- ²⁵ B. M. McCoy and T. T. Wu, *The Two-Dimensional Ising Model* (Harvard University Press, Cambridge, MA, 1973).
- ²⁶ L. Onsager, Phys. Rev. **65**, 117 (1944).
- ²⁷ C. N. Yang, Phys. Rev. **85**, 809 (1952).
- ²⁸ B. M. McCoy and T. T. Wu, Phys. Rev. **162**, 463 (1967).
- ²⁹ D. B. Abraham and F. Latrémolière, Phys. Rev. E **50**, R9 (1994).
- ³⁰ H. E. Stanley, *Introduction to Phase Transitions and Critical Phenomena* (Oxford University Press, New York, 1971).
- ³¹ M. N. Barber, in *Phase Transitions and Critical Phenomena*, edited by C. Domb and J. L. Lebowitz (Academic, London, 1983), Vol. 8.
- ³² C. Domb, in *Phase Transitions and Critical Phenomena*, edited by C. Domb and J. L. Lebowitz (Academic, London, 1974), Vol. 3.
- ³³ P. C. Hohenberg and B. Halperin, Rev. Mod. Phys. **49**, 435 (1977).
- ³⁴ K. Binder, in *Phase Transitions and Critical Phenomena*, edited by C. Domb and J. L. Lebowitz (Academic, London, 1976), Vol. 5.
- ³⁵ J. D. Gunton, M. S. Miguel, and P. S. Sahni, in *Phase Transitions and Critical Phenomena*, edited by C. Domb and J. L. Lebowitz (Academic, London, 1983), Vol. 8.
- ³⁶ H. M. Duiker and P. D. Beale, Phys. Rev. B **41**, 490 (1990).
- ³⁷ P. D. Beale, Integrated Ferroelectrics **4**, 107 (1994).
- ³⁸ H.-B. Braun, Phys. Rev. Lett. **71**, 3557 (1993); J. Appl. Phys. **75**, 4609 (1994); Phys. Rev. B **50**, 16485 (1994); **50**, 16501 (1994).
- ³⁹ A. Zangwill, *Physics at Surfaces* (Cambridge University Press, Cambridge, 1988).
- ⁴⁰ For reviews of thin films, see e.g. L. M. Falicov et al., J. Mater. Res. **5**, 1299 (1990); R. Allenspach, J. Magn. Magn. Mater. **129**, 160 (1994); H.-J. Elmers, Int. J. Mod. Phys. B **9**, 3115 (1995).
- ⁴¹ P. W. Selwood, *Chemisorption and Magnetization* (Academic, New York, 1975).
- ⁴² H. Bu, C. D. Roux, and J. W. Rabalais, J. Chem. Phys. **97**, 1465 (1992).
- ⁴³ A. Grossman, W. Erley, and H. Ibach, Surf. Sci. **337**, 183 (1995).
- ⁴⁴ M. Voetz, H. Niehus, and J. O’Connor, Surf. Sci. **292**, 211 (1993).
- ⁴⁵ F. M. Leibsle, Surf. Sci. **297**, 98 (1993).
- ⁴⁶ C. Klink, L. Olesen, and F. Besenbacher, Phys. Rev. Lett. **71**, 4350 (1993).
- ⁴⁷ C. Klink, I. Stensgaard, and E. Laengsgaard, Surf. Sci. **342**, 250 (1995).
- ⁴⁸ D. R. Mullins, D. R. Huntley, and S. H. Overbury, Surf. Sci. **323**, L287 (1995).
- ⁴⁹ N. Memmel, G. Rangelov, and E. Bertel, Phys. Rev. B **43**, 6938 (1991).
- ⁵⁰ J. C. Hamilton and T. Jach, Phys. Rev. Lett. **46**, 745 (1981).
- ⁵¹ M. S. Dresselhaus, Nature **292**, 196 (1981).
- ⁵² A. S. Mosunov, O. P. Ivanenko, and M. V. Kuvankin, Vacuum **43**, 785 (1992).
- ⁵³ A. Goursot et al., Int. J. Quantum Chem. **48**, 277 (1993).
- ⁵⁴ See e.g. P. V. Hendriksen, S. Linderoth, and P.-A. Lindgård, Phys. Rev. B **48**, 7259 (1993); P. V. Hendriksen, S. Linderoth, and P.-A. Lindgård, J. Phys.: Cond. Matter **5**,

- 5675 (1993); L.-J. Zhou, X. G. Gong, Q. Q. Zheng, and C. Y. Pan, cond-mat/9606031 (unpublished); and references therein.
- ⁵⁵ See, e.g., C. Salling, S. Schultz, I. McFadyen, and M. Ozaki, *IEEE Trans. Magn.* **27**, 5184 (1991); V. I. Safarov et al., *Micros. Microanal. Microstruct.* **5**, 381 (1994); M. W. J. Prins et al., *Appl. Phys. Lett.* **64**, 1207 (1994); M. W. J. Prins, R. H. M. Groeneveld, D. L. Abraham, and H. van Kempen, *Appl. Phys. Lett.* **66**, 1141 (1995); R. Wiesendanger et al., *Phys. Rev. Lett.* **65**, 247 (1990); R. Wiesendanger, *J. Magn. Soc. Jpn.* **18**, 4 (1994); R. Wiesendanger, *Jpn. J. Appl. Phys.* **34**, 3388 (1995); A. L. V. de Parga and S. F. Alvarado, *Phys. Rev. Lett.* **72**, 3726 (1994); E. Betzig et al., *Appl. Phys. Lett.* **61**, 142 (1992); and T. J. Silva, S. Schultz, and D. Weller, *Appl. Phys. Lett.* **65**, 1658 (1994).
- ⁵⁶ Y. Martin and H. K. Wickramasinghe, *Appl. Phys. Lett.* **50**, 1455 (1987); D. Sarid, *Scanning Force Microscopy with Applications to Electric, Magnetic, and Atomic Forces* (Oxford University Press, New York, 1991); P. Grütter, H. J. Mamin, and D. Rugar, in *Scanning Tunneling Microscopy*, edited by R. Wiesendanger and H.-J. Güntherodt (Springer, New York, 1992), Vol. 2.
- ⁵⁷ T. Chang, J.-G. Zhu, and J. H. Judy, *J. Appl. Phys.* **73**, 6716 (1993).
- ⁵⁸ Y. Luo and J.-G. Zhu, *IEEE Trans. Magn.* **30**, 4080 (1994).
- ⁵⁹ N. S. Wei and S. Y. Chou, *J. Appl. Phys.* **76**, 6679 (1994).
- ⁶⁰ R. O'Barr, M. Lederman, S. Schultz, W. Xu, A. Scherer and R. J. Tonuci, *J. Appl. Phys.* **79**, 5303 (1996).
- ⁶¹ W. Wernsdorfer, B. Doudin, D. Maily, K. Hasselbach, A. Benoit, J. Meier, J.-Ph. Ansermet and B. Barbara, *Phys. Rev. Lett.* **77**, 1873 (1996).
- ⁶² H. Yang, Z. Wang, L. Song, M. Zhao, J. Wang and H. Luo, *J. Phys. D: Appl. Phys.* **29**, 2574 (1996).
- ⁶³ M. Lederman, G. A. Gibson, and S. Schultz, *J. Appl. Phys.* **73**, 6961 (1993).
- ⁶⁴ M. Lederman, D. R. Fredkin, R. O'Barr, S. Schultz and M. Ozaki *J. Appl. Phys.* **75**, 6217 (1994).
- ⁶⁵ M. Lederman, S. Schultz, and M. Ozaki, *Phys. Rev. Lett.* **73**, 1986 (1994).
- ⁶⁶ W. Wernsdorfer, K. Hasselbach, D. Maily, B. Barbara, A. Benoit, L. Thomas and G. Suran, *J. Magn. Magn. Mater.* **140-144**, 389 (1995).
- ⁶⁷ W. Wernsdorfer, K. Hasselbach, D. Maily, B. Barbara, A. Benoit, L. Thomas and G. Suran, *J. Magn. Magn. Mater.* **145**, 33 (1995).
- ⁶⁸ W. Wernsdorfer, K. Hasselbach, A. Benoit, G. Cernicchiaro, D. Maily, B. Barbara and L. Thomas *J. Magn. Magn. Mater.* **151**, 38 (1995).
- ⁶⁹ W. Wernsdorfer, K. Hasselbach, A. Sulpice, A. Benoit, J.-E. Wegrove, L. Thomas, B. Barbara and D. Maily, *Phys. Rev. B* **53**, 3341 (1996).
- ⁷⁰ R. M. H. New, R. F. W. Pease, R. L. White, *J. Vac. Sci. Technol. B* **13**, 1089 (1995); R. M. H. New, Ph.D. dissertation, Stanford University, 1995; R. M. H. New, R. F. W. Pease, R. L. White, R. M. Osgood and K. Babcock, *J. Appl. Phys.* **79**, 5851 (1995).
- ⁷¹ For reviews, see K. Binder, in *Phase Transitions and Critical Phenomena*, edited by C. Domb and J. L. Lebowitz (Academic, London, 1983), Vol. 8; and K. Binder, in *Polarized Electrons in Surface Physics*, edited by R. Feder (World Scientific, Singapore, 1985).
- ⁷² For a review, see D. B. Abraham, in *Phase Transitions and Critical Phenomena*, edited by C. Domb and J. L. Lebowitz (Academic, London, 1986), Vol. 10.

- ⁷³ E. Köster and T. C. Arnoldussen, in *Magnetic Recording*, edited by C. D. Mee and E. D. Daniel (McGraw-Hill, New York, 1987), Vol. 1, p. 98.
- ⁷⁴ S. Mørup, *Hyperfine Interactions* **90**, 171 (1994).
- ⁷⁵ U. Nowak, *IEEE Trans. Magn.* **31**, 4169 (1995).
- ⁷⁶ N. Metropolis et al., *J. Chem. Phys.* **21**, 1087 (1953).
- ⁷⁷ R. J. Glauber, *J. Math. Phys.* **4**, 294 (1963); M. Suzuki and R. Kubo, *J. Phys. Soc. Jpn.* **24**, 51 (1968).
- ⁷⁸ P. A. Martin, *J. Stat. Phys.* **16**, 149 (1977).
- ⁷⁹ A. B. Bortz, M. H. Kalos, and J. L. Lebowitz, *J. Comp. Phys.* **17**, 10 (1975).
- ⁸⁰ For a discussion on the equivalence of the dynamics produced by these two algorithms, see M. A. Novotny, *Computers in Physics* **9**, 46 (1995).
- ⁸¹ H. Tomita and S. Miyashita, *Phys. Rev. B* **46**, 8886 (1992).
- ⁸² P. A. Rikvold, H. Tomita, S. Miyashita, and S. W. Sides, *Phys. Rev. E* **49**, 5080 (1994).
- ⁸³ For some recent results relevant to the validity of this approximation for systems with *conserved* order parameter, see B. Krishnamachari, J. McLean, B. Cooper, and J. P. Sethna, preprint cond-mat/9605142, *Phys. Rev. B* in press.
- ⁸⁴ R. A. Ramos, S. W. Sides, P. A. Rikvold, and M. A. Novotny, in preparation.
- ⁸⁵ J. S. Langer, *Ann. Phys. (N.Y.)* **41**, 108 (1967); *Phys. Rev. Lett.* **21**, 973 (1968); *Ann. Phys. (N.Y.)* **54**, 258 (1969).
- ⁸⁶ N. J. Günther, D. A. Nicole, and D. J. Wallace, *J. Phys. A* **13**, 1755 (1980).
- ⁸⁷ K. Leung and R. K. P. Zia, *J. Phys. A* **23**, 4593 (1990).
- ⁸⁸ K. Binder, *Z. Phys. B* **43**, 119 (1981).
- ⁸⁹ K. Binder, *Phys. Rev. A* **25**, 1699 (1982).
- ⁹⁰ B. Berg, U. Hansmann, and T. Neuhaus, *Z. Phys. B* **90**, 229 (1993).
- ⁹¹ J. Lee, M. A. Novotny, and P. A. Rikvold, *Phys. Rev. E* **52**, 359 (1995).
- ⁹² I. M. Lifshitz, *Sov. Phys. JETP* **15**, 939 (1962).
- ⁹³ S. K. Chan, *J. Chem. Phys.* **67**, 5755 (1977).
- ⁹⁴ S. M. Allen and J. W. Cahn, *Acta Metall.* **27**, 1085 (1979).
- ⁹⁵ J. A. N. Filipe, A. J. Bray, and S. Puri, *Phys. Rev. E* **52**, 6082 (1995).
- ⁹⁶ A. N. Kolmogorov, *Bull. Acad. Sci. USSR, Mat. Ser.* **1**, 355 (1937).
- ⁹⁷ W. A. Johnson and P. A. Mehl, *Trans. Am. Inst. Mineral Mining Eng.* **135**, 365 (1939).
- ⁹⁸ M. Avrami, *J. Chem. Phys.* **7**, 1103 (1939); **8**, 212 (1940); **9**, 177 (1941).
- ⁹⁹ R. A. Ramos, P. A. Rikvold, and M. A. Novotny, in *Physical Phenomena at High Magnetic Fields*, edited by Z. Fisk, L. Gorkov, D. Meltzer and R. Scriver, (World Scientific, Singapore, 1995), p. 380.
- ¹⁰⁰ S. W. Sides, R. A. Ramos, P. A. Rikvold, and M. A. Novotny, in preparation.
- ¹⁰¹ E. Ising, *Z. Phys.* **31**, 253 (1925).
- ¹⁰² K. Huang, *Statistical Mechanics*, 2. ed. (Wiley, New York, 1987), p. 363.
- ¹⁰³ T. Young, *Phil. Trans. R. Soc. London* **95**, 65 (1805).
- ¹⁰⁴ For reviews of wetting phenomena see: S. Dietrich, in *Phase Transitions and Critical Phenomena*, edited by C. Domb and J. L. Lebowitz (Academic, London, 1988), Vol. 12.
- ¹⁰⁵ D. B. Abraham, *Phys. Rev. Lett.* **44**, 1165 (1980).
- ¹⁰⁶ W. Selke, *J. Stat. Phys.* **56**, 609 (1989).
- ¹⁰⁷ A. Maciolek, *J. Phys. A* **29**, 3837 (1996).
- ¹⁰⁸ The function $\text{ARCTAN}(x, y)$ used here is known in FORTRAN as $\text{arctan2}(x, y)$. It is also

included in the programming language Mathematica as ArcTan[x,y] [S. Wolfram, Mathematica: A System for Doing Mathematics by Computer, Second Edition, (Addison-Wesley, Reading, MA, 1990)].

¹⁰⁹ J. Lothe and G. M. Pound, J. Chem. Phys. **36**, 2080 (1962).

¹¹⁰ The prefactor exponent K consists of two parts: $K = b + c$. The exponent b is universal, independent of the dynamics, and expected to be 1 for $d=2$ ^{85,86} and $-7/3$ for $d=3$.⁸⁶ The exponent c is part of the “dynamic prefactor” and is expected to equal 2 for dynamics that can be represented by a Fokker-Planck equation,⁸⁵ such as a local Monte Carlo algorithm with updates at randomly chosen sites.⁸² Strictly speaking, it is not correct to include c into the “complete” free-energy barriers $\widehat{\Delta F}$. However, since the full value of K contributes to the nucleation time, we do so here for convenience.

¹¹¹ C. Kittel, Introduction to Solid State Physics, Sixth Edition, (Wiley, New York, 1986), p. 426.

TABLES

TABLE I. The length ℓ used in Eq. (16) to calculate H_{ThSp} . The listed value of τ indicates the waiting time for which the Thermodynamic Spinodal was fitted to the peak in H_{sw} vs. L .

T/J	τ [MCSS]	ℓ
0.65	10^7	1.0(1)
1.30	4×10^3	1.4(2)
1.81535	10^2	2.0(4)

FIGURES

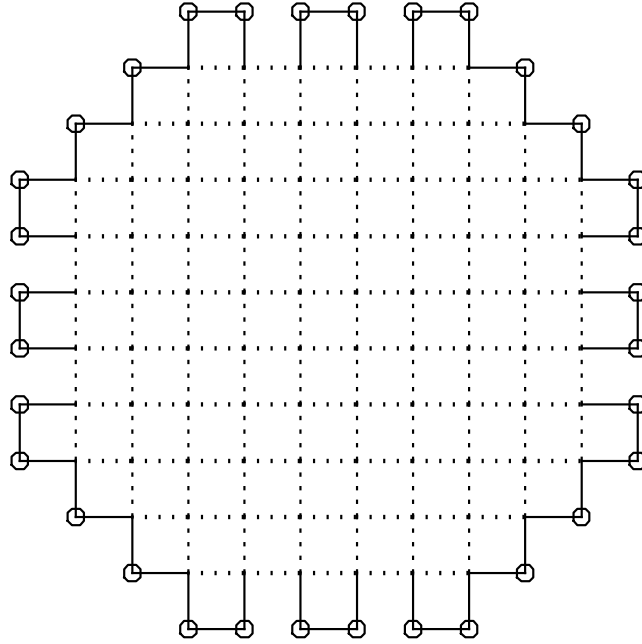


FIG. 1. An octagon of diameter $L = 12$. Surface sites, which contribute to the sum \sum_{i_Σ} in Eq. (5), are circled. Surface bonds, which contribute to the sum $\sum_{\langle i,j \rangle_\Sigma}$ in Eq. (5), are shown as solid lines. In Eq. (3), all sites contribute to the sum \sum_i and both boundary bonds and bulk bonds (dotted lines) contribute to the sum $\sum_{\langle i,j \rangle}$.

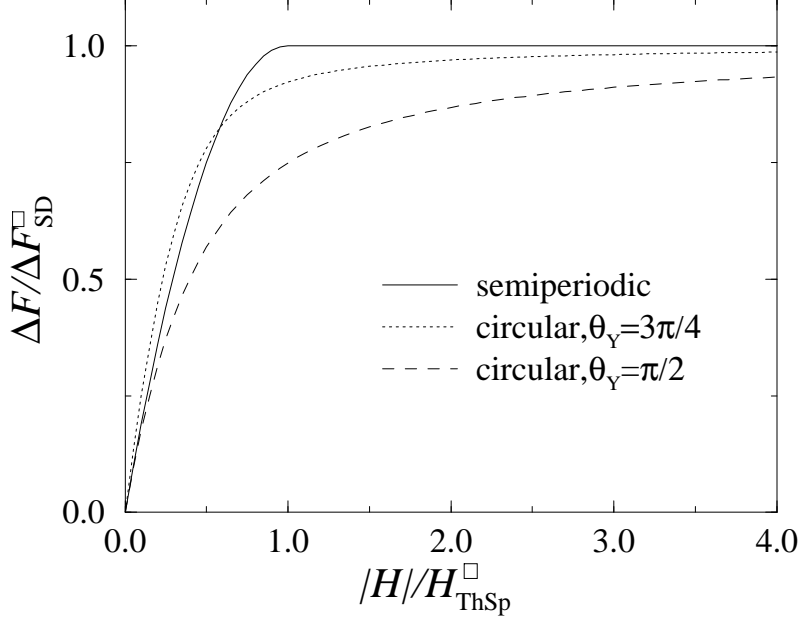


FIG. 2. The normalized free-energy barriers (neglecting entropic corrections for the size dependent number of nucleation sites) for semiperiodic [$\Delta F^\square/\Delta F_{SD}^\square$, solid curve, Eq. (37)] and circular [$\Delta F^\circ/\Delta F_{SD}^\square$, dotted and dashed curves, Eq. (48)] systems. The curve for periodic systems [$\Delta F/\Delta F_{SD}$ vs. $|H|/H_{ThSp}$, Eq. (19)] coincides with the result for semiperiodic systems shown here. Note that the scaling variable $|H|/H_{ThSp}^\square$ differs from the scaling variable $x = L/2R_c$ in Eq. (48) only by a factor dependent on the contact angle θ_Y . Thus, with θ_Y and the magnetic field kept constant, these plots can be regarded as functions of the system size in units of the critical droplet diameter [see Eqs. (20), (38) and (48b)].

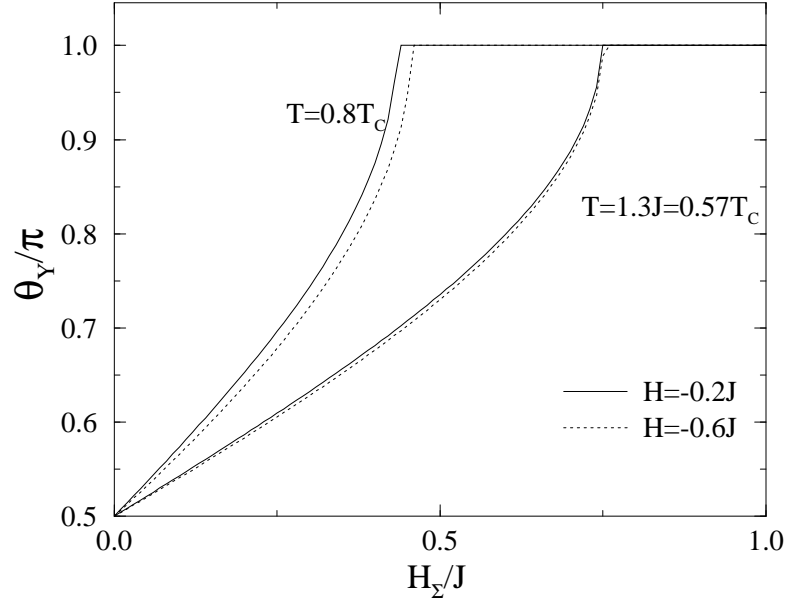


FIG. 3. The contact angle θ_Y as a function of the boundary field H_Σ for two different values of H and T . These plots are approximations calculated from Eqs. (26) and (27). Note that these (negative) values of H do not significantly influence the contact angle. This approximation gives an idea of the contact angles produced by the surface field H_Σ in our Monte Carlo simulations in semiperiodic systems. Because of the different topology, this approximation may not be equally good for octagonal lattices.

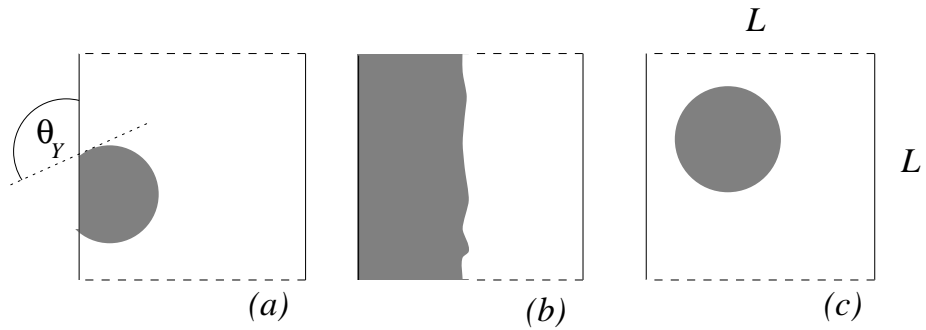


FIG. 4. Three situations which may lead to the nucleation of a critical fluctuation in a semiperiodic system: (a) a droplet at the boundary (the contact angle θ_Y [given by Eq. (27)] is shown), (b) the slab configuration, (c) a droplet in the bulk. The dashed lines represent edges of the system that are connected by periodic boundary conditions. The linear system size is L in both directions.

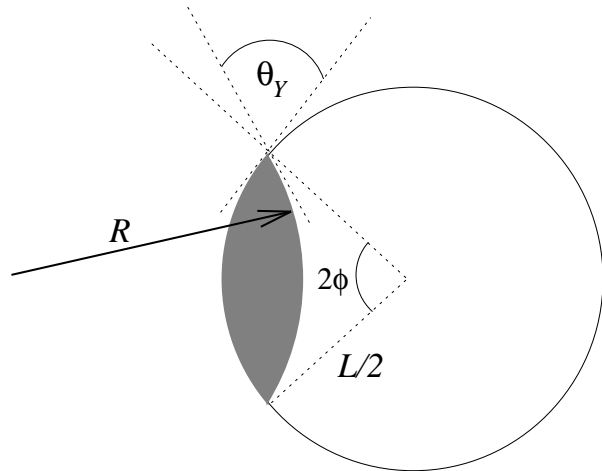


FIG. 5. The contact angle θ_Y and the “angular diameter” 2ϕ of a droplet nucleating at the boundary of a circular system. R denotes the radius of the inner surface of the droplet, and L is the diameter of the circular system.

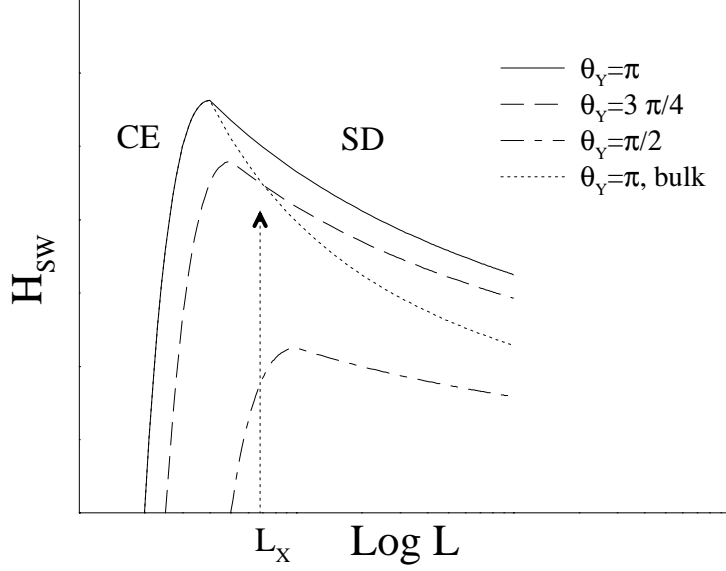


FIG. 6. An illustration of the theoretical results for the influence of θ_Y on the L dependence of the switching field. The solid and dashed curves correspond to surface nucleation; the dotted curve corresponds to bulk nucleation. For $\theta_Y = \pi$, bulk nucleation is dominant everywhere in the SD regime. For $\theta_Y = 3\pi/4$, surface nucleation dominates in the SD regime for $L \leq L_x$, but for $L > L_x$ bulk nucleation becomes dominant. For $\theta_Y = \pi/2$, surface nucleation dominates throughout the SD region. Note the following: (i) larger values of θ_Y produce more dramatic increases of H_{sw} with L in the CE region; (ii) larger values of θ_Y produce more clearly pronounced peaks of H_{sw} vs. L with larger values of H_{sw} at the peak; (iii) the effect of bulk nucleation is to make the peak appear more pronounced. The curves were obtained by numerically solving for H using Eqs. (36), (49) and (50) for a fixed waiting time; both the parameters and the curves are in quantitative agreement with Fig. 7a.

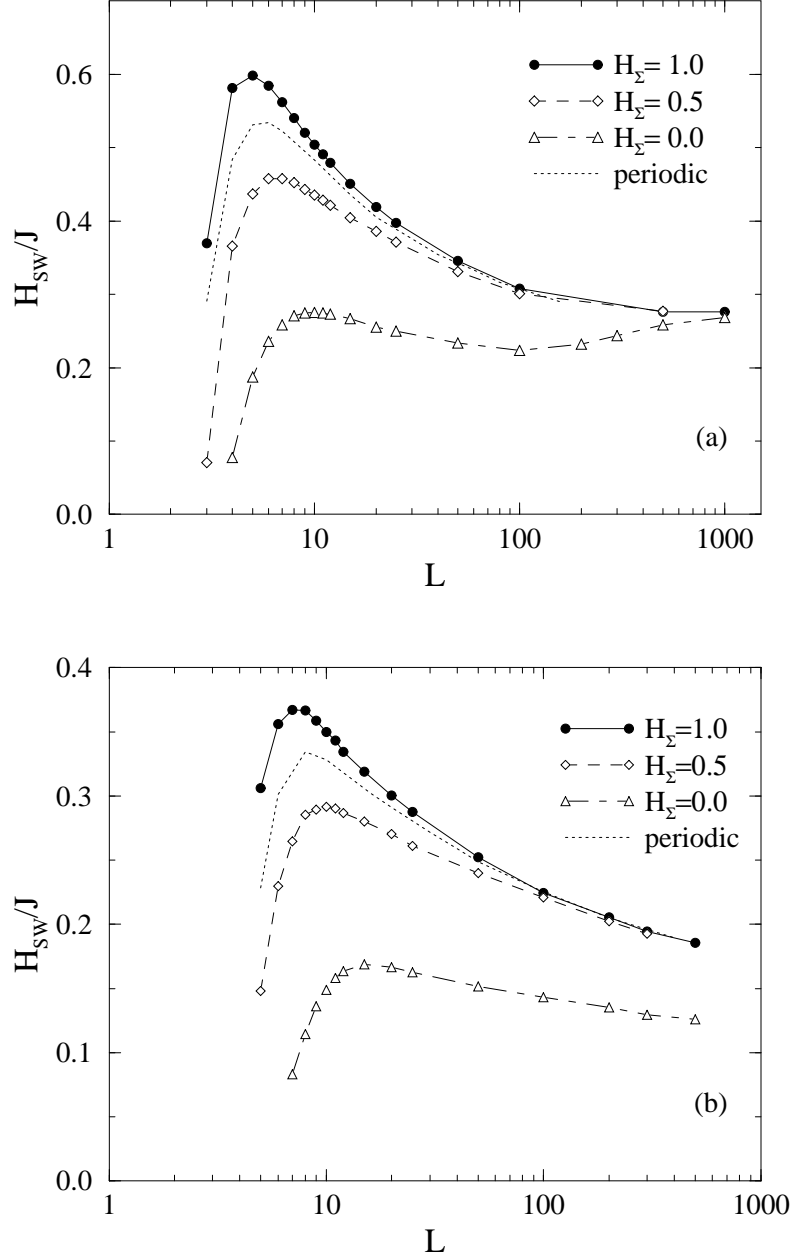


FIG. 7. The switching field H_{sw} as a function of system size L for various values of H_Σ in semiperiodic systems at $T = 1.3J \approx 0.57T_c$. Data for periodic systems are shown as dotted lines. (a) $\tau = 1000$ MCSS. (b) $\tau = 30000$ MCSS. Note the similarity in shape of the measured switching fields to the droplet-theory predictions presented in Fig. 6.



FIG. 8. Snapshots of Monte Carlo simulations for semiperiodic systems. Panel (a) shows a supercritical droplet nucleated at the boundary of a system with $L = 10$, and panel (b) shows a droplet nucleated in the interior of a system with $L = 50$. In both cases, $T = 1.3J$, $H_\Sigma = 0.5J$, and for each system size, the magnetic field H is chosen equal to the switching field for $\tau = 1000$. Thus, the snapshots correspond to data points shown in Fig. 7(a). The smaller system ($L = 10$) is clearly in the “boundary dominated” single-droplet regime. The larger system ($L = 50$) is already in the crossover regime to “bulk dominated” nucleation, where the probability of observing a droplet nucleating at the boundary is smaller. For even larger systems with $L \approx 100$, almost all droplets nucleate in the bulk.

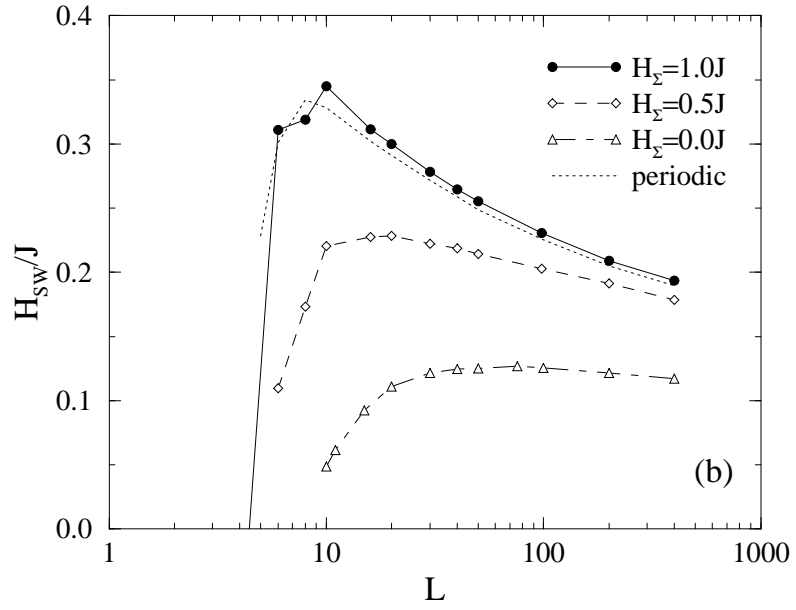
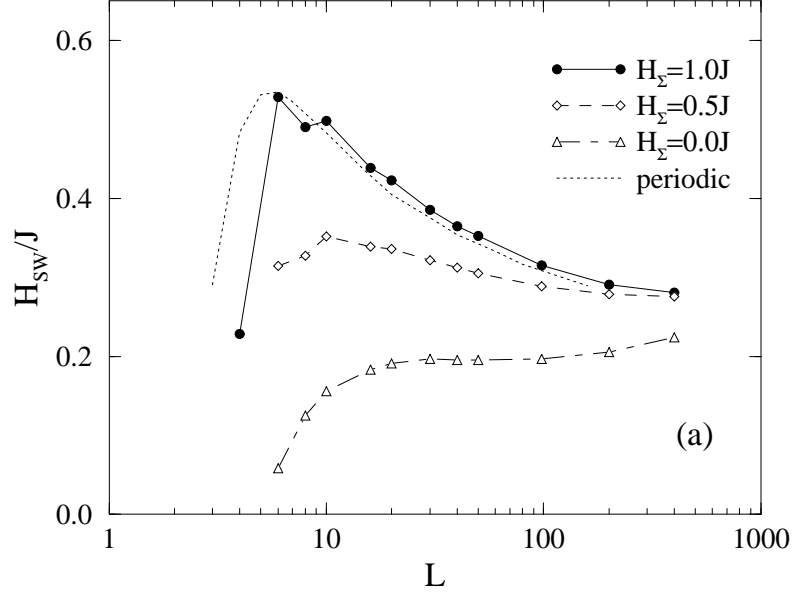


FIG. 9. The switching field H_{sw} as a function of system size L for various values of H_Σ for circular systems at $T = 1.3J \approx 0.57T_c$. Data for periodic systems are shown as dotted lines. (a) $\tau = 1000$ MCSS. (b) $\tau = 30000$ MCSS.

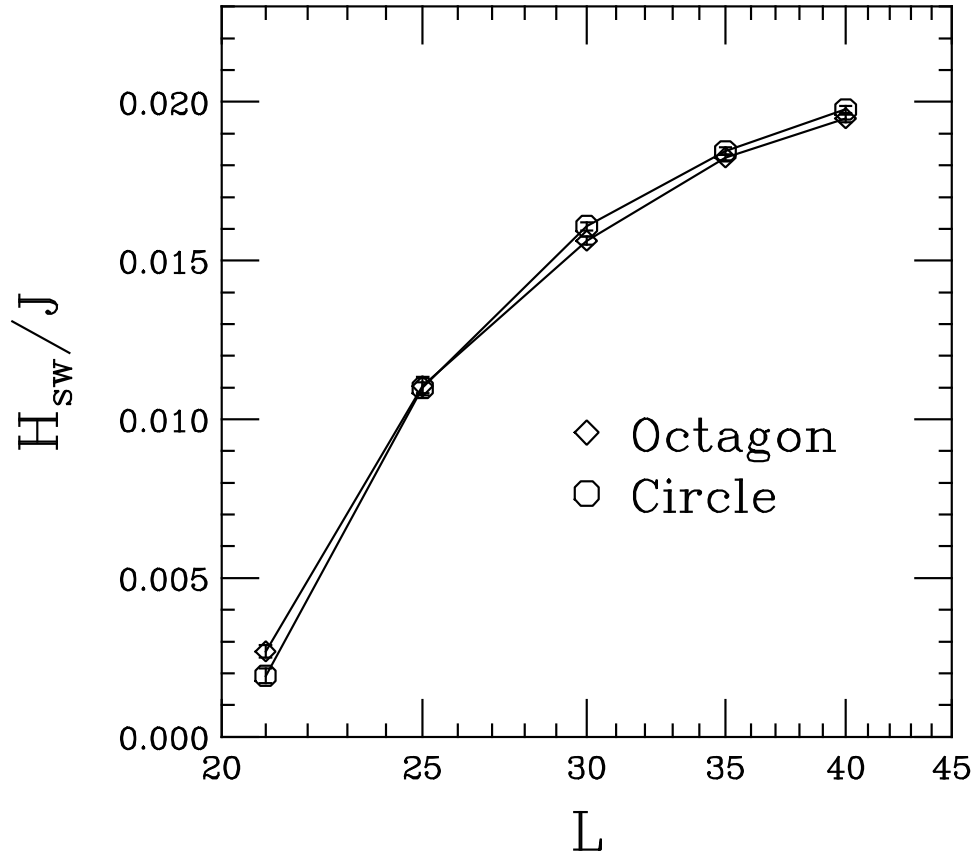


FIG. 10. The switching field as a function of system size for small octagonal and circular systems with $T=0.9T_c$, $\tau=2000$ MCSS, and $H_\Sigma = J_\Sigma = 0$.

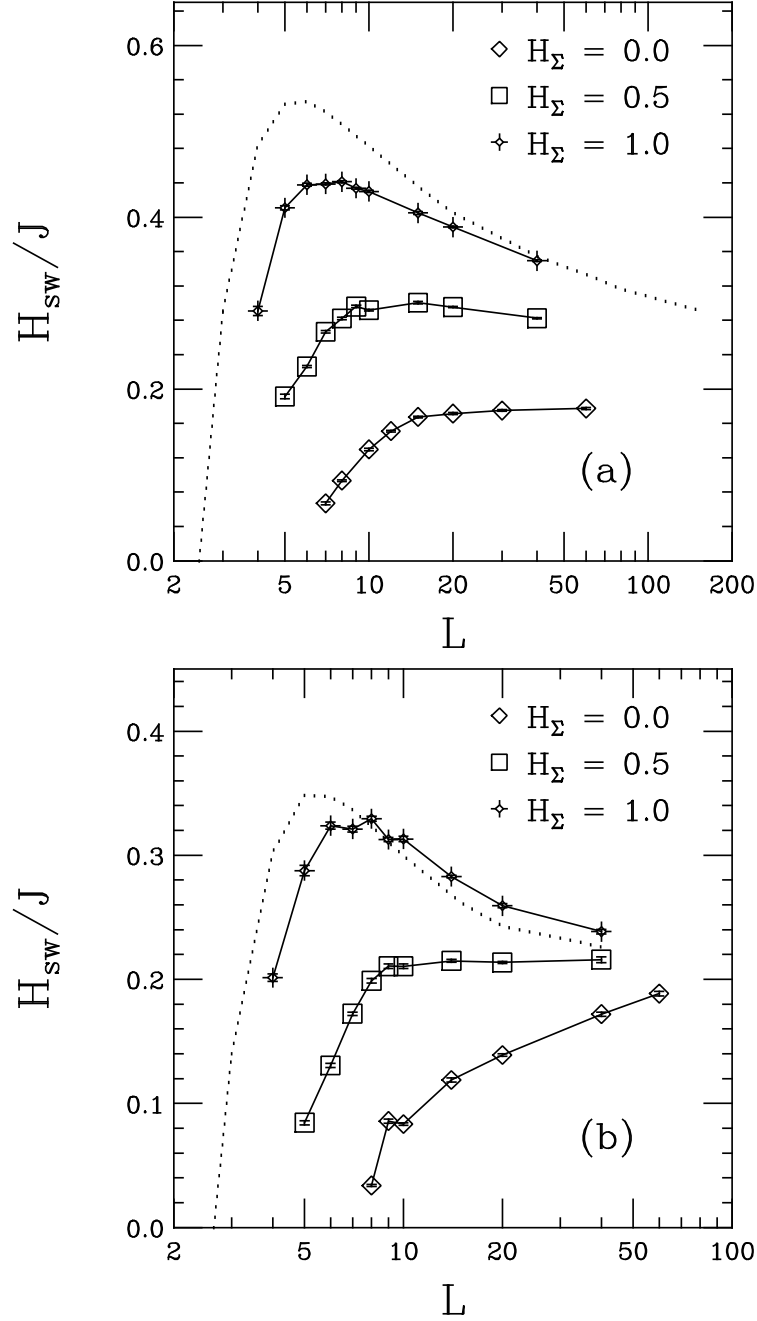
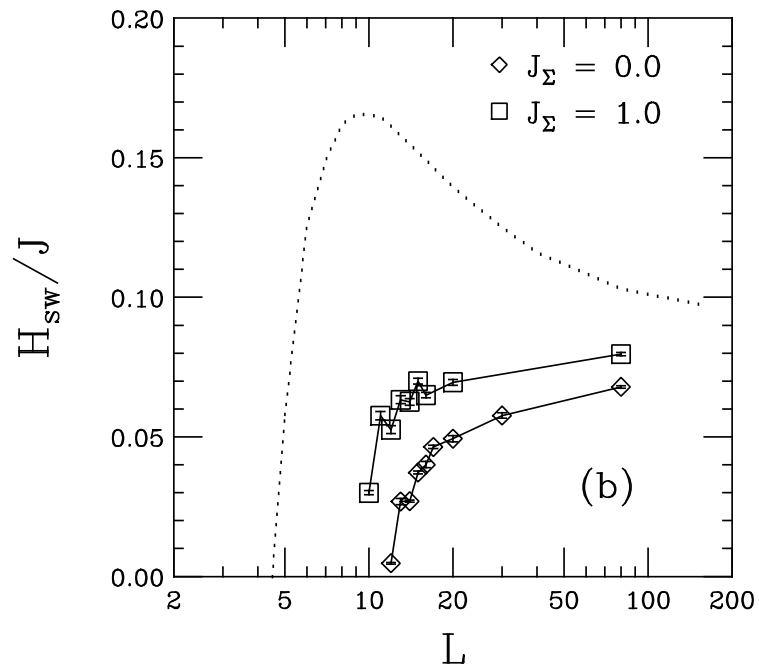
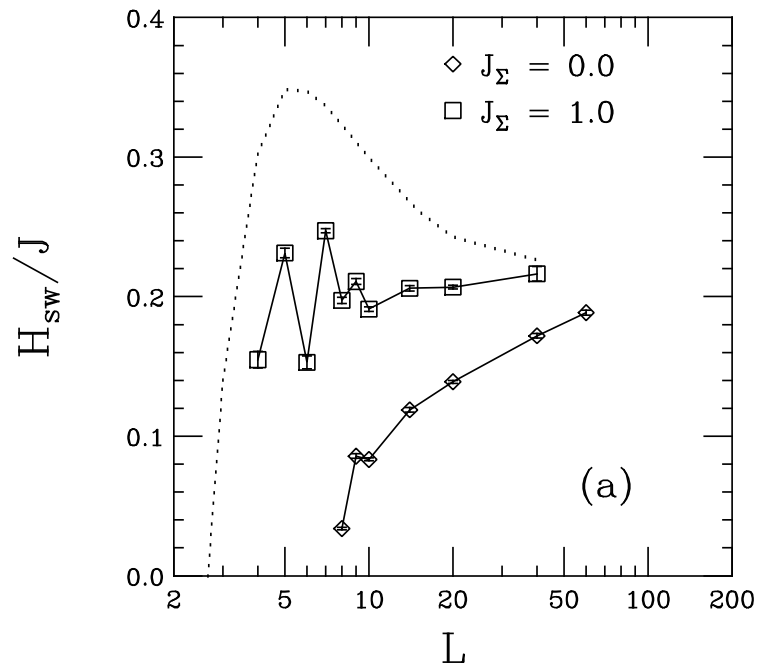


FIG. 11. The switching field as a function of system size for octagonal systems with various values of H_Σ . Data for periodic systems (dotted lines) were taken from Ref. 4. (a) $T = 1.3J \approx 0.57T_c$ and $\tau = 1000$ MCSS. (b) $T = 0.8T_c \approx 1.81J$ and $\tau = 100$ MCSS.



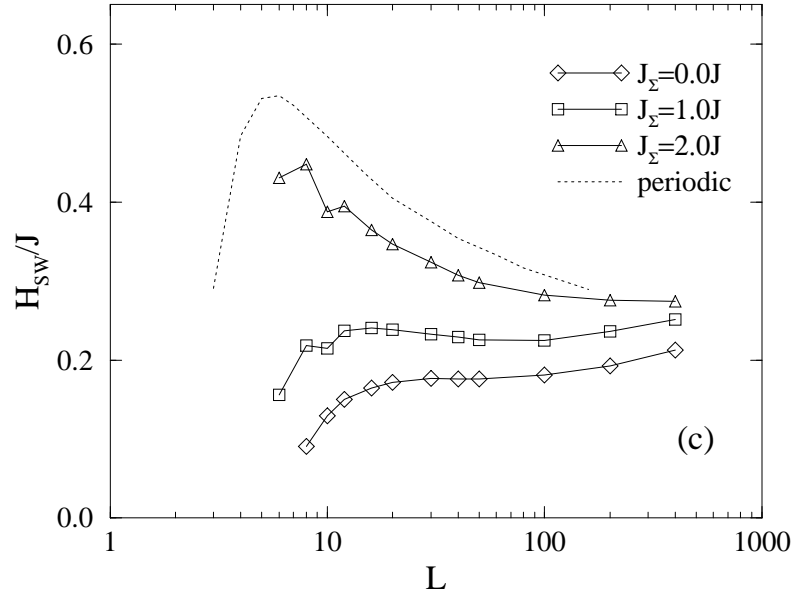


FIG. 12. The switching field as a function of system size for various values of J_{Σ} for octagonal systems. (a) $\tau=100$ MCSS, $T=0.8T_c \approx 1.81J$. (b) $\tau=1000$ MCSS, $T=0.8T_c \approx 1.81J$. (c) $\tau=1000$ MCSS, $T=1.3J \approx 0.57T_c$.

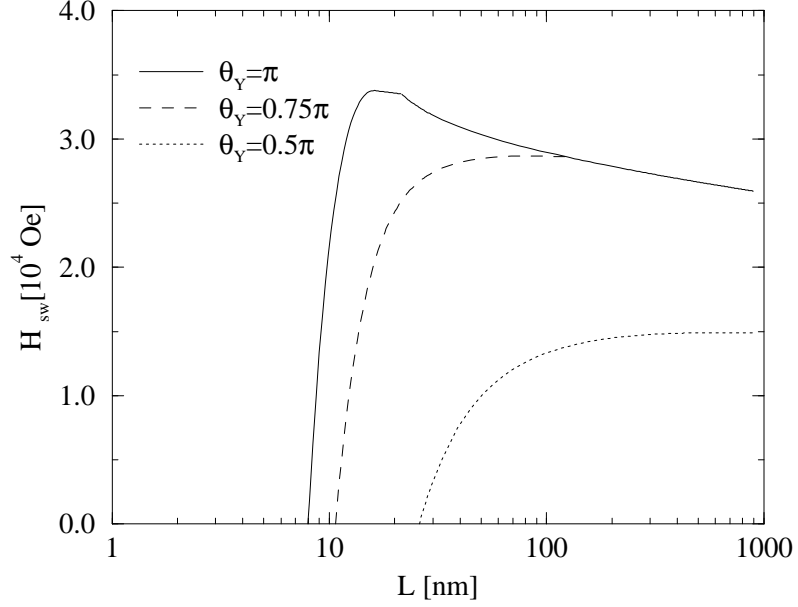


FIG. 13. Droplet-theory predictions for the switching fields vs. system size for a hypothetical ferromagnetic monolayer with $T_c = 375$ K, magnetic moment of a single atom of 1 Bohr magneton, and lattice constant 0.3 nm. According to Eqs. (3-5) in Ref. 7, such a system is expected to be single-domain if it is smaller than 400 nm. The three curves shown correspond to system boundaries with different properties characterized by the contact angle θ_Y of the stable-phase droplets at the system boundary. We note that the crossover between the regime with droplets nucleating at the system boundary and the regime with bulk nucleation, as it was described in this work, is observed for the two upper curves.